Modeling of a Turbulent Line Vortex

Larry A. Young[‡]
NASA Ames Research Center, Moffett Field, CA, 94035-1000

There is considerable interest in turbulence modeling of vortical structures. The most fundamental of all such structures is the line, or columnar, vortex. Many laminar flow solutions of line vortices have been reported in the literature. Only a few analytical treatments have been presented for turbulent line vortex modeling. More contemporary predictive work has focused on performing highly refined higher-order CFD predictions of vortices for specific areas of interest -- in particular, examining wing/blade-tip trailed vortex roll-up or far-field wake temporal evolution. In almost all cases, the turbulence closure models are not necessarily well suited for the high gradients and rotational effects typical of wing/rotor trailed tip vortices. Recently, though, there have been a number of computational studies of turbulent vortices that have adopted highly sophisticated direct numerical simulations of the unsteady Navier-Stokes momentum equations. This work in particular has been very promising in terms of understanding not only the mean flow behavior of turbulent vortices but their higher-modal characteristics as well. Nonetheless, there remains much still to learn about turbulent vortices in general. In particular, the transition flow mechanism from laminar to fully turbulent vortex states is still largely undetermined. A new analytical approach is suggested in this paper. The result is progress towards a turbulent line vortex model that captures many of the flow features previously observed, predicted, and/or conjectured about this fundamental building block of the vortical fluid flow, including, most importantly, the transition from laminar to turbulent flow states.

Nomenclature

$r^\bullet$	Nondimensional radial coordinate, $r^\bullet = r/r_{c0}$
r_{c0}	"Finite core" vortex filament core size radius (at time equal to zero), m
Re	Vortex Reynolds number, $\mathrm{Re} = \gamma/\nu$
$t^\bullet$	Nondimensional time parameter, $t^\bullet = \nu t/r_{c0}^2$
$\mathbf{V}$	Velocity vector, cylindrical coordinates, $\mathbf{V} = \begin{bmatrix} v_r & v_\theta & v_z \end{bmatrix}$, m/sec
$v_\theta^\bullet$	Nondimensional tangential velocity, $v_\theta^\bullet = r_{c0} v_\theta/\gamma$
$z^\bullet$	Nondimensional axial coordinate, $z^\bullet = z/r_{c0}$
γ	Vortex filament initial circulation strength, m^2/sec
ν	Kinematic viscosity, m^2/sec
θ	Angular coordinate, radians
$\boldsymbol{\omega}$	Vorticity vector, $\boldsymbol{\omega} = \begin{bmatrix} \omega_r & \omega_\theta & \omega_z \end{bmatrix}$, 1/sec

[‡] Aerospace Engineer, Aeromechanics Branch, Flight Vehicle Research and Technology Division, Mail Stop 243-12, AIAA Associate Fellow.

I. Introduction

THE formation and evolution of vortices shed/trailed from fixed- and rotary-wing aircraft continues to be an area of considerable research interest. Despite the advance of sophisticated and computationally intensive analysis tools, the study of these fundamental vortical fluid flow structures is, as yet, still incomplete. The study of line vortices reaches back over a century of investigation – originating with the pioneering work of Helmholtz, Kelvin, Rankine, Lamb, Oseen, and many others (for surveys of this classic work, see Refs. 1-2, for example). Still progress made in this area, though substantial, has also been comparatively slow. Turbulent vortical flow structure consequently remains an active area of research investigation. Recently, investigations carried out with variants of DNS (Direct Numerical Simulation) and LES (Large Eddy Simulation) Navier-Stokes CFD (Computational Fluid Dynamics) solutions have, in particular, begun to shed some light upon some of the remaining ill-understood issues regarding the evolution of turbulent vortices and other vortical structures (e.g. Ref. 3).

Why is this still an important area of investigation from an engineering perspective, though? Even with the advances made possible with modern computational power, there is still much to learn. First of all, an improved understanding of vortical flow structures continues to be essential for the understanding of the aerodynamic performance of aerial vehicles and, therefore, their design. Many comprehensive engineering analyses for rotary-wing aerial vehicles, for example, are still based upon free-wake predictions incorporating fairly simple vortex models that derive considerable heritage from classic work in laminar vortex solutions. CFD-based predictions of aerial vehicle wake structures are rapidly superceding free-wake predictions, but there are still significant limitations/trade-offs required in terms of grid resolution and accounting for numerical/artificial dissipation effects influencing the predicted spatiotemporal evolution of the trailed tip vortices and other vortical structures in the rotary-wing wake. Second, the transition flow mechanisms from laminar to fully turbulent vortex states are still poorly understood for trailed vortices. Laminar to turbulent vortex transition is a particularly crucial issue for the emerging field of rotary-wing UAVs and/or the proper interpretation and application of small-scale model rotor data to full-scale vehicles. Third, the theoretically most accurate current means of predicting vortex evolution, DNS and LES Navier-Stokes CFD solutions, are still prohibitively expensive in terms of time and computational resources to be directly applied on a routine basis to engineering design and analysis problems. There must, instead, be some efficient means of capturing the essential flow behavior from these sophisticated but computationally expensive CFD investigations and arriving at refined engineering-analysis-compatible vortex models for pragmatic design and development problems.

The intent of this paper is, therefore, to undertake the study of turbulent line vortices by means of an approximate but analytical treatment versus a wholly computational/numerical study.

II. Initial Analysis Framework

The analysis presented in this paper builds upon earlier work related to deriving exact analytical solutions for a small family of laminar columnar (line) vortices as well as additional work detailing an approximate three-dimensional analysis technique applicable to the unsteady viscous Helmholtz vorticity transport equation, referred to as the length scale factor (LSF) methodology, Refs. 4-7.

Earlier work presented in Refs. 4-5 detailed the derivation and predicted results, respectively, of an exact Navier-Stokes solution for a laminar columnar vortex having an initially uniform vorticity distribution. This particular solution is an independently derived, mathematically distinct, alternate solution to the Ref. 8 work, also derived for an initially uniform vorticity distribution. Each version, Ref. 4-5 versus Ref. 8, has its own relative strengths and weaknesses, but, for most part, the Ref. 4-5 solution is of greater generality. In both cases a laminar line vortex model is described whereby the unsteady solutions go from a Rankine-like tangential velocity profile to one that is nearly identical to the Lamb-Oseen vortex, see Fig. 1. There are several different laminar vortex models detailed in the literature. This particular vortex model was chosen to represent the laminar basic flow state for this paper's analysis because of its quasi-separable analytic nature and because it was also an unsteady solution (refer to Eq.

88b, Appendix B). An alternate family of vortices, as detailed in Ref. 6, could also potentially be employed as a laminar basic flow state.

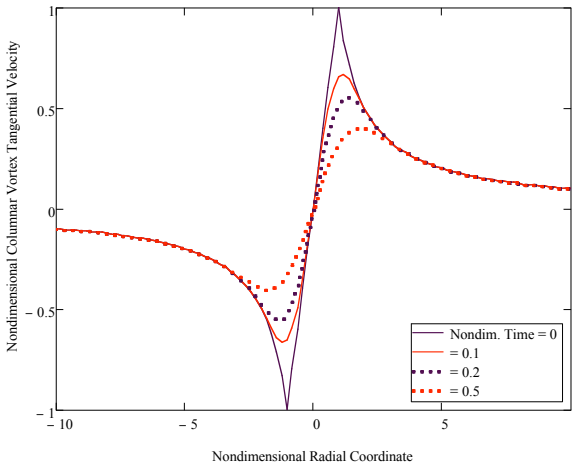

Fig. 1 – Laminar/Basic Flow Solution for a Line Vortex with Initially Uniform Vorticity

Unlike the classic turbulent flow approach taken with Navier-Stokes Reynolds-averaging, e.g. Ref. 11, the velocity will be expressed as follows in terms of both the laminar unsteady flow solution (defined in terms of the v_r, v_θ, and v_z velocity components) and turbulent fluctuation velocity components by $\hat{v}_r$, $\hat{v}_\theta$, and $\hat{v}_z$ (this alternate approach being more inspired, instead, by the classic treatment for fluid flow stability theory, e.g. Refs. 11-12, for disturbance velocities). This reflects the interpretation of the turbulent flow problem as a fluctuation between two flow states, one flow state being the earlier derived unsteady laminar flow solution.

$$\mathbf{V} = \begin{bmatrix} v_r + \hat{v}_r & v_\theta + \hat{v}_\theta & v_z + \hat{v}_z \end{bmatrix} \tag{1}$$

In turn, that also implies (principally as a consequence of the length-scale factor methodology relating the axial and radial vorticity to the axial and radial velocity components) that the vorticity can be similarly expressed in terms of both a laminar, but unsteady, basic flow solution and turbulent fluctuation vorticity components.

$$\boldsymbol{\omega} = \begin{bmatrix} \omega_r + \hat{\omega}_r & \omega_\theta + \hat{\omega}_\theta & \omega_z + \hat{\omega}_z \end{bmatrix} \tag{2}$$

The LSF methodology, in general, seeks to derive approximate, but fully three-dimensional and unsteady, solutions to the viscous Helmholtz vorticity transport equations by employing length scale factors to establish simple linear relationships between either two or three velocity/vorticity pairs. These length scale factor relationships can be applied to either to the basic flow or to disturbance velocities, in the case of nonlinear stability analysis, or, for turbulent flow analysis, to the turbulent fluctuation velocity components. By further making the large-Reynolds-number assumption for the flow problem, approximate analytical solutions can be derived. For the analysis outlined in this paper, it is unnecessary to apply the LSF methodology to the laminar basic flow. Instead, the length scale factors are applied only to the turbulent fluctuation velocities, such that

$$\begin{aligned} \hat{v}_z &= -\ell \hat{\omega}_z \\ \hat{v}_r &= -\ell \hat{\omega}_r \\ \hat{v}_\theta &= -\ell \hat{\omega}_\theta \end{aligned} \tag{3a-c}$$

This work is very analogous to earlier work, Ref. 7, discussing vortex filament nonlinear stability subject to various active flow control strategies seeking to disrupt the basic flow state of the vortex.

Given the above LSF relationships, an analysis is provided by which "disturbance velocity" -type equations (drawing upon stability analysis heritage) are derived, see Eq. 4a-c. Instead of using these disturbance-type equations to assess the stability of the basic flow, the equations are employed to directly solve for analytic expressions for the columnar/line vortex turbulent fluctuation velocities.

$$\ell^{\bullet}\frac{\partial \omega_z^{\bullet}}{\partial r^{\bullet}}\hat{v}_r^{\bullet}-\frac{v_\theta^{\bullet}}{r^{\bullet}}\frac{\partial \hat{v}_z^{\bullet}}{\partial \theta}-\ell^{\bullet}\omega_z^{\bullet}\frac{\partial \hat{v}_z^{\bullet}}{\partial z^{\bullet}}=0$$

$$\frac{v_\theta^{\bullet}}{r^{\bullet}}\frac{\partial \hat{v}_r^{\bullet}}{\partial \theta}+\ell^{\bullet}\omega_z^{\bullet}\frac{\partial \hat{v}_r^{\bullet}}{\partial z^{\bullet}}=0$$

$$\frac{v_\theta^{\bullet}}{r^{\bullet}}\frac{\partial \hat{v}_\theta^{\bullet}}{\partial \theta}-\hat{v}_r^{\bullet}\frac{\partial v_\theta^{\bullet}}{\partial r^{\bullet}}+\ell^{\bullet}\omega_z^{\bullet}\frac{\partial \hat{v}_\theta^{\bullet}}{\partial z^{\bullet}}=0$$

(4a-c)

The complete unsteady solution is obtained from the combination of two solutions – one for the mean flow state (both laminar and turbulent) and the other for the "turbulent fluctuation" flow. These solutions are detailed in Appendices A-B. In Appendix C, an analysis and discussion is presented as to the level of approximation inherent in applying the LSF linear vorticity and velocity relationships as given Eq. 3a-c.

III. Predicted Turbulent Vortex Phenomenology

The derived turbulent model is a fully unsteady solution. The turbulent fluctuation solutions are derived first. The mean flow solution is subsequently derived. Finally, a solution for effective vortex "accelerated aging" is derived and its implications on both the mean and the fluctuation flow are considered. However, for the solution to be complete, it must employ a prescribed initial laminar vortex flow model. Several laminar vortex flow models could be used to prescribe the basic flow state of the analysis. For the representative results presented in this paper, a "uniform-core" laminar vortex model is employed; refer to Refs. 4-5 and Appendix B for details. The instantaneous turbulent flow is three-dimensional in nature. For example, helical isosurface structures wrapped along the turbulent vortex axis are predicted, though not graphically presented, in this paper. The analytical solution, though derived primarily within a deterministic framework, has incorporated into it an essential stochastic character. For example, it is shown that only through elements of such stochastic functionality is a net nonzero mean flow predicted for the turbulent vortex tangential velocity profile. Perhaps one of the most intriguing aspects of the derived model is that it captures the vortex transition from laminar to turbulent flow states. Further, it also predicts a "relaminarization" process for turbulent vortices in the late stages of their evolution. The term relaminarization is used in this paper solely in the context that the vortex turbulent kinetic energy (TKE) reaches some maximum and then decreases with time.

Both the transition from laminar to turbulent flow states, and the subsequent vortex relaminarization after being fully turbulent, can be clearly seen in Fig. 2. Figure 2 shows the trend with nondimensional time of the peak (at or near the vortex centerline) TKE of the vortex (refer to Eq. 62g, Appendix A). Such a relaminarization process is implicit in the vortex turbulence measurements of several different experimental studies reported in the literature – including Refs. 16-17. In Fig. 2 a rapid transition from laminar to turbulent flow begins at very small values of nondimensional time. The TKE reaches a maximum with fully-developed turbulence and then subsequently begins to relaminarize at a comparatively slow pace.

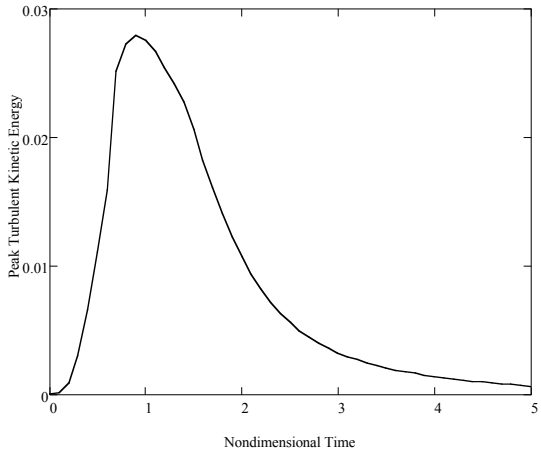

Fig. 2 – Transition from Laminar to Turbulent Flow with Subsequent Relaminarization

Figures 3-8 describe the general mean flow characteristics of the modeled turbulent line vortex. Figure 1 illustrated the time dependence of the laminar vortex tangential velocity profile. Figure 3 presents a comparable set of mean flow tangential velocity profiles for a turbulent line vortex (refer to Eqs. 10a and 60, Appendix A). Note that the vortex can only be considered fully turbulent for the two oldest vortex profiles shown. The profiles corresponding to the two smallest values of nondimensional time are in a state of transitional flow. The analysis includes a "cutoff" constant to show where/how the profile should jump from a $1/r^{\beta}$ behavior, where $\beta < 1$, reflecting the influence of turbulence on the mean flow, to a $1/r$ profile to reflect the correct far-field potential flow like behavior. The jump from a turbulent $1/r^{\beta}$ profile to a potential far-field $1/r$ profile can be clearly seen in the profiles corresponding to the smallest values of nondimensional time. At these small values in time the profiles still represent transitional flow and therefore the asymptotic approach to the potential $1/r$ profile is accomplished further inward to the core than it is for the later vortex ages, where the vortices reflect full-developed turbulence.

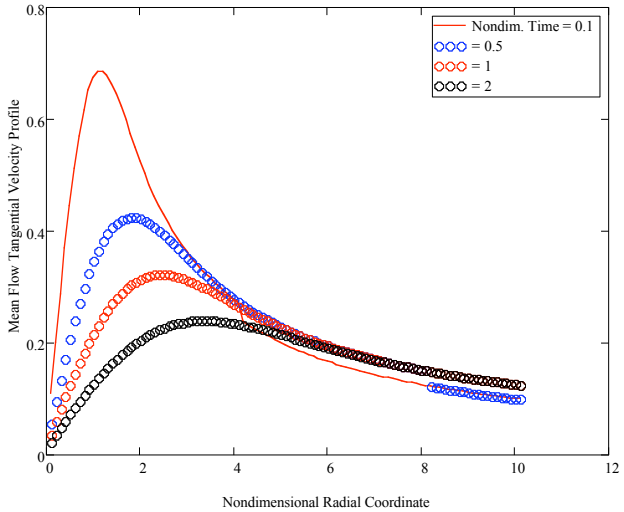

Fig. 3 – Tangential Velocity Mean Flow Profile

A general comparison of the non-normalized laminar versus turbulent mean flow tangential velocity profiles is shown in Fig. 4 for an equivalent value of nondimensional time. The turbulent vortex has been subjected to accelerated aging, thereby leading to great effective diffusion of the vortex than is the case for the laminar vortex. This accelerated aging of the turbulent vortex results in a more rapid decrease in the

peak tangential velocities with time as well as increased rate of growth of the vortex core radius as compared to laminar vortices. This is a well-known mean flow behavior of turbulent vortices, Refs. 16-19 and 25-26. The general form of the two profiles is also different, though perhaps subtly so in the particular velocity profiles presented. The turbulent vortex is more rounded about, and after, the vortex peak than the laminar vortex. In this regards, the predicted turbulent tangential velocity profile is consistent with experimental observations and other analytical models and computational studies. However, a comparison between normalized laminar and turbulent tangential velocity profiles, wherein the velocities are divided by the peak velocity and the radial coordinate divided by the core radius, reveals that turbulent mean flow tangential velocity profile needs to be shifted further outward from the vortex core. This will be discussed further shortly.

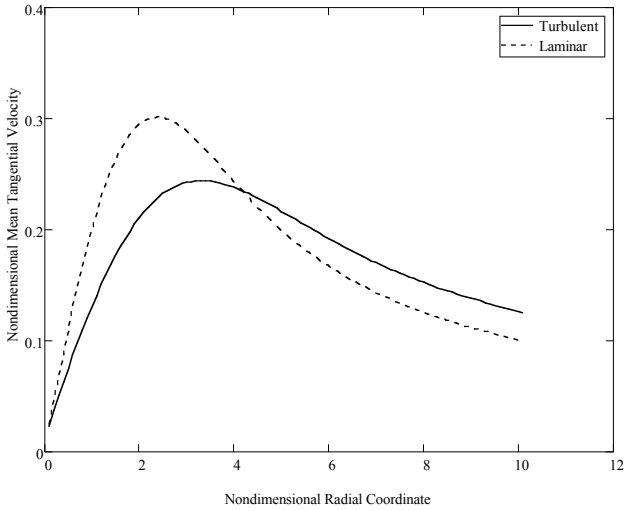

Fig. 4 – Tangential Velocity Mean Flow Profiles

Turbulent vortices have a higher normalized tangential velocity mean flow profile for the outer region, beyond the vortex, as compared to any laminar vortex, particularly for that of a Lamb-Oseen vortex profile. This can be clearly seen in Fig. 5.

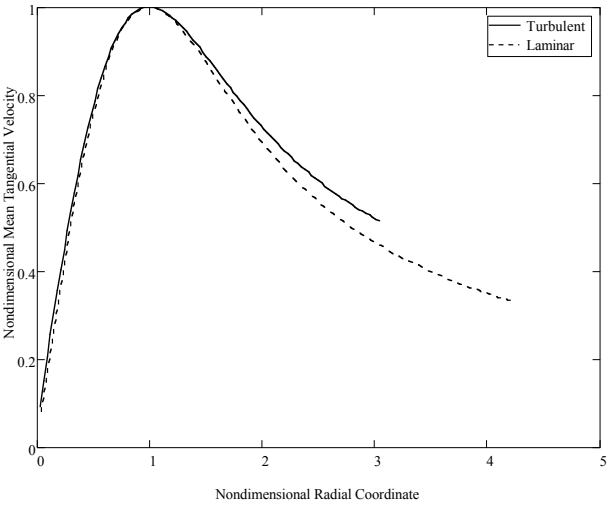

Fig. 5 – Normalized Comparison between Lamb-Oseen Vortex and Turbulent Vortex Model

In addition to the mean flow tangential velocity profiles, Figs. 6-7 illustrate the time dependence of the vortex core radii and the peak tangential velocity for the turbulent vortex. As noted earlier, they both reveal significant and expected differences in their trends with respect to time as compared to fully laminar line vortices. The relative magnitude of those predicted differences is a function of certain key modeling parameters and constants, which are only partially defined in the analysis, as discussed in detail in Appendix A. Note that relaminarization has already begun narrowing the relative differences between the Figs. 6 and 7 laminar and turbulent vortex core size and peak tangential velocity trends at large values of nondimensional time.

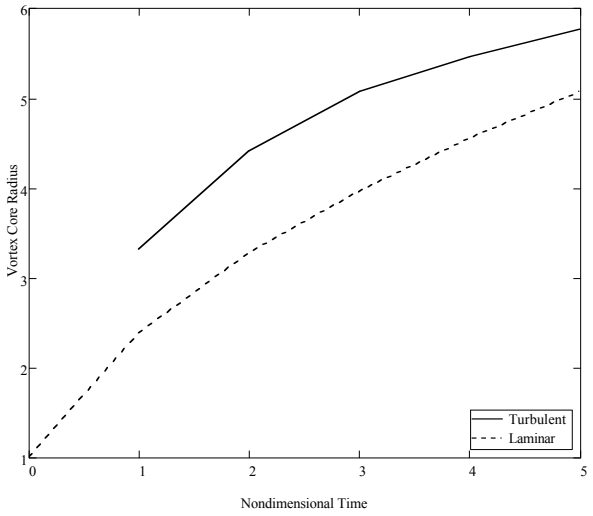

Fig. 6 – Laminar versus Turbulent Vortex Core Radii Time Dependence

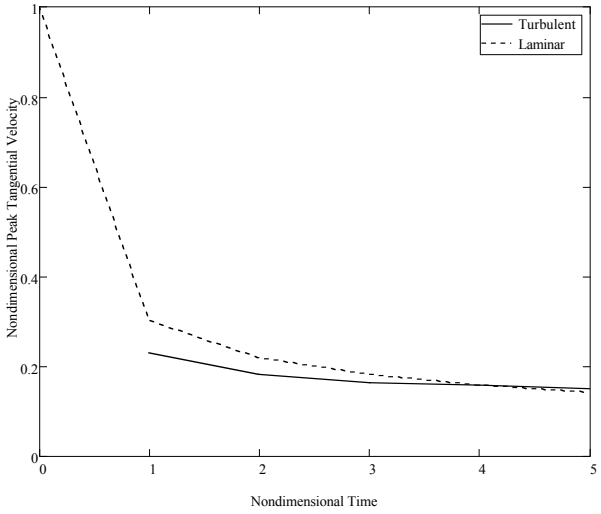

Fig. 7 – Peak Tangential Velocity Time Dependence

A representative vortex circulation distribution is shown in Fig. 8. The difference between the laminar and turbulent circulation profiles is not because of some difference in the analytic character in the two distributions, but is instead merely a consequence of the accelerated vortex aging for turbulent vortices (refer to Eq. 72, Appendix A). The circulation profile is still very much laminar-like in nature. For example, there is no prediction of a "circulation overshoot" as first predicted/hypothesized in Ref. 24 and discussed in other works.

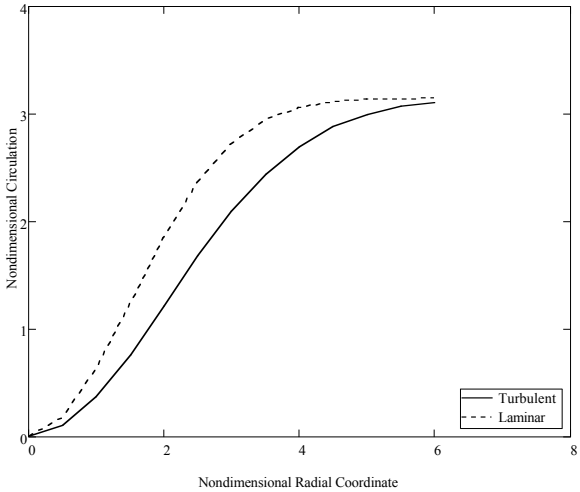

Fig. 8 – Laminar vs. Turbulent Vortex Circulation Distribution

Perhaps the greatest utility, and most novel nature, of the current analysis is in its treatment of vortex turbulence prediction. A direct analytical assault to derive solutions for the turbulent fluctuations themselves has been attempted. The governing equations for this problem are summarized in Eqs. 3a-c. These turbulent fluctuation governing equations are analogous to disturbance velocity equations used in classic flow stability analyses. The mean flow solution is, in some regards, merely a consequence of the derived turbulent fluctuation solutions. General trends in vortex turbulence, Reynolds stress, and TKE are predicted in Figs. 9-12 (Eq. 62a-h, Appendix A). These trends are qualitatively in good agreement with the experimental vortex turbulence measurements, e.g. Refs. 16-19 and 25-26. The radial and tangential turbulence profiles reach a maximum at or near the vortex center. Alternatively, the axial turbulence is at a minimum at the vortex center. The predicted axial turbulence, though, is significantly lower in overall magnitude, as compared in relation to the radial and tangential turbulence, than is indicated in most experimental data. This is undoubtedly a consequence of most experimental measurements being made for trailed vortices versus a line vortex. Trailed vortices have a significant amount of nonzero mean axial flow inside the vortex core. Reference 18 attempted to simulate a line vortex using steady axial flow injection into a trailed vortex core; such an experimental simulation of a line vortex appeared to reduce the magnitude of the axial turbulence as compared to a trailed vortex without injection. In this regards, Ref. 18 axial turbulence results were somewhat more consistent with the predictions of this paper.

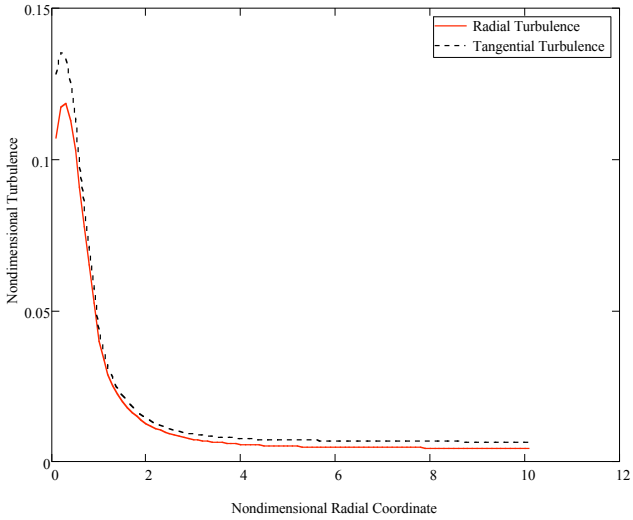

Fig. 9 – Radial and Tangential Turbulence Radial Distributions

Note the small anisotropy of the radial versus tangential velocity turbulence profiles. This anisotropy is intrinsically linked to the fluctuation skew, or offset, essential for establishing a nonzero net mean flow for the tangential velocity profile, as compared to the radial and axial mean flow distributions, which average out to zero net flow. The recent experimental work of Ref. 17 highlighted the importance of being able to model this anisotropy between the two turbulence components. The "dimples" seen at $r^{\bullet} \to 0$ for the radial and tangential velocity turbulence profiles may have some physicality. There is some experimental evidence, again as seen in Ref. 17, for such a small drop-off in turbulence at the vortex center for the radial and tangential turbulence profiles, but it is a small, secondary effect at best. Alternatively, such drop-offs in the radial and tangential turbulence profiles could simply be an artifact of the numerical difficulty of estimating asymptotic limits of the two turbulence profiles so close to the vortex center.

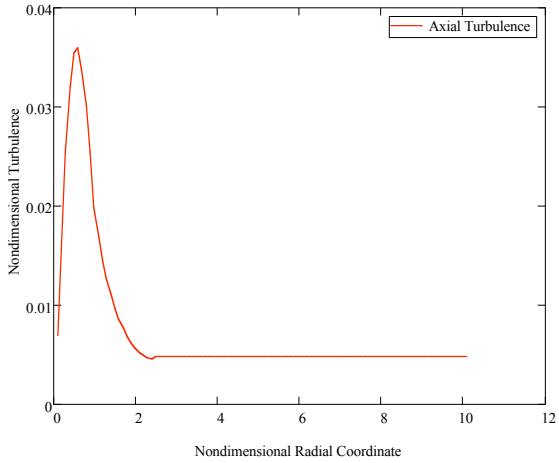

Fig. 10 – Axial Turbulence Radial Distribution (for a Line Vortex)

Reynolds shear stress predictions are extremely difficult to measure as well as predict. Figure 11 illustrates some general radial distribution trends for this paper's predicted Reynolds shear stresses. Higher-mode contributions to the predicted Reynolds shear stress profiles can be discerned in Fig. 11, i.e. the slight "bumps" around $r^{\bullet} \approx 1$, but for the most part these profiles are dominated by the lower modes.

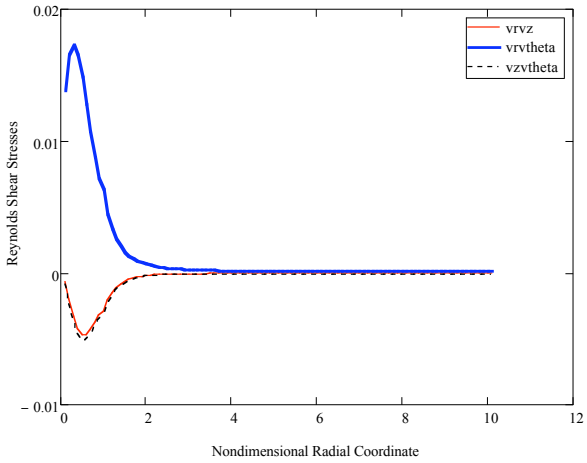

Fig. 11 – Predicted Reynolds Shear Stress Radial Distributions

The relative contribution of higher-modes to the vortex Reynolds shear stresses is as yet undecided. The experimental work of Ref. 17 would suggest that the lower modes, like the predictions provided in this

paper, dominate the Reynolds stress distributions. However, though the accuracy of Ref. 18 results is somewhat questionable, the experimental measurements of Ref. 18 seem to show more of a contribution for the higher-modes.

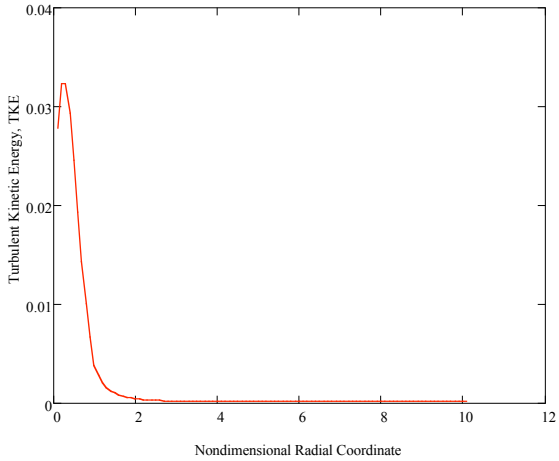

Fig. 12 – Turbulent Kinetic Energy Radial Distribution

These initial results are only qualitative, the vortex model currently only being phenomenological in nature, and not really predictive in a quantitative sense.[§] More work needs to be performed to ideally extend the analysis and to rigorously derive the constants/parameters used in the analysis.

IV. Limitations of Analysis and Future Opportunities

The derived analysis does not directly address the circumstances in which vortex formation from a wing- or blade-tip occurs as an initially turbulent flow process. Such a circumstance might be tackled by considering only that portion of the vortex evolution solution wherein the vortex is fully turbulent. Finally, also unaddressed by this analysis is the influence of external strain fields on vortex evolution. Such external strain fields are an important consideration for vortex evolution in rotary-wing wakes. It is, however, straightforward to apply the turbulent flow analysis outlined in Appendix A to other laminar/basic-flow vortex models besides the uniform-core model summarized in Appendix B. For example, the same analysis can be applied to the parabolic-core model detailed in Refs. 4-5 or the family of unsteady laminar vortices detailed in Ref. 6.

The normalized energy spectrum for the turbulent vortex model, as a function of mode number, is presented in Fig. 13. The total energy for each mode has been estimated by integrating across the vortex, from $0 \le r^{\bullet} < \infty^{-}$. A considerable amount of research has been directed at examining the energy spectrum of various different turbulent flows, with the expectation, for the most part, that the energy spectrum in the inertial range will approach some sort of "universal" scaling.

[§] The key parameter and constant values used in the above figures are as follows (unless otherwise noted): $\eta = 10$, $\vartheta = 0.5$, $\alpha = 10^{-11}$, $t^{\bullet} = 1$, and $t^{\bullet}_{eff} = 1.93$, among others. Their definition, interdependencies, and general constraints are detailed in the appendices.

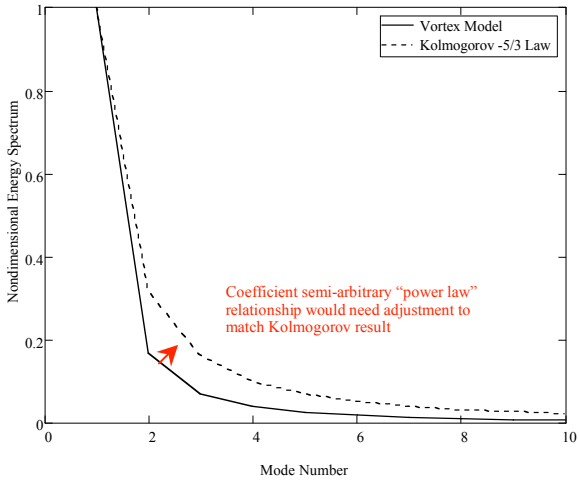

Fig. 13 – Predicted Energy Spectrum

It can be seen from Fig. 13 that the energy spectrum for the current predictions presented shows a steeper fall-off of energy with mode number than the classic Kolmogorov -5/3 law for isotropic turbulence in the inertial range, Ref. 15. This partially explains why very little higher-mode contribution is seen in the turbulence and Reynolds shear stress predictions of Figs. 9-12. An energy spectrum more reflective of the Kolmogorov spectrum would exhibit more in the way of higher-mode contributions than currently being demonstrated in the predictions. This discrepancy in the energy spectrum is only of minor consequence. It would be straightforward, if need be, to tailor the higher-mode constants employed in the analysis to match the Kolmogorov -5/3 power law for the turbulence energy spectrum.

Finally, the derived analysis suggests a possible explanation for the dichotomy of why certain laminar flows, when subjected to flow stability analysis, analytically appear stable to two-dimensional and sometimes three-dimensional excitation (this includes the work of Ref. 7) even though clearly, through experimental demonstrations, the flows can indeed transition into turbulent states. Examples of this dichotomy include the Lamb-Oseen vortex, which has been subjected to numerous stability analyses, e.g. Ref. 28, that have consistently failed to show amplified instabilities that could lead to turbulence. The answer, as suggested by the analysis provided in this paper, lies in the fact that the flow solution can be considered "superposed" in nature. In this context, the laminar solution terms can be nominally independent of, but additive to, the turbulent terms in some complete solution, i.e. the two solutions are superposed. Therefore the laminar solution may be stable, when subjected to flow stability analysis, but the superposed turbulent analytical contribution would obviously be unstable in a general sense. Indeed, it would only be the inherent transitional nature of some previously-not-derived hidden, or meta, flow state of a turbulent fluctuation solution that yields fully turbulent flow. One such superposed laminar/turbulent flow solution has been derived for line vortices in this paper.

Concluding Remarks

A preliminary analytical treatment is developed that provides new insights into turbulent vortex evolution. It represents a significant departure from previous work in the literature and provides a conjectural and analytical framework that addresses still little understood aspects of turbulent vortex phenomenology. The derived turbulent vortex model is a hybrid stochastic/deterministic solution. For example, a novel result of the work is the modeling of vortex transition from laminar to turbulent flow states. Additionally, another novel aspect of the work is the modeling of a relaminarization process for turbulent vortices.

Considerable work remains to advance this vortex model into a fully predictive tool. In particular, a rigorous methodology to define several key parameters/constants in the model still needs to be developed. Many of these parameters/constants are currently defined only in an informal and/or conjectural manner. Nonetheless, the analysis already shows considerable promise in that it embodies a host of rich yet-to-be-fully-explored mathematical and physical concepts and insights for vortical flow modeling.

Though the problem considered, that of turbulent line vortices only, might seem overly simplistic, it is anticipated that the results of this analysis will have implications for the analysis of more general/complex vortical flow phenomena.

References

[1]Lamb, H., Hydrodynamics, Sixth Edition, Dover Publications, New York.

[2]Saffman, P.G., Vortex Dynamics, Cambridge University Press, 1992.

[3]Duraisamy, K. and Lele, S.K., "DNS of Temporal Evolution of Isolated Turbulent Vortices," Center for Turbulence Research: Proceedings of the Summer Program 2006, Stanford, CA, 2006.

[4]Young, L.A., "Vortex Flow Behavior Subsequent to Perpendicular Collision with a Solid Body," Soon to be published NASA TM.

[5]Young, L.A., "Influence of Initial Vorticity Distribution on Axisymmetric Vortex Breakdown and Reconnection," AIAA-2007-1283, AIAA Aerospace Sciences Meeting, Reno, NV, January 8-11, 2006.

[6]Young, L.A., "A Family of Vortices to Study Axisymmetric Vortex Breakdown and Reconnection," 25th AIAA Applied Aerodynamics Conference, Miami, FL, June 25-28, 2007.

[7]Young, L.A., "Vortex Filament Evolution Subject to Pulsed/Periodic Disruption," AIAA-2008-0367, AIAA Aerospace Sciences Meeting, Reno, NV, January 7-10, 2008.

[8]Aboelkassem, Y., Vatistas, G.H., and Esmail, N., "Viscous Dissipation of Rankine Vortex Profile in Zero Meridional Flow," Acta Mechanica Sinica, Vol. 21, November 21, 2005, pp. 550-556.

[9]Carslaw, H.S. and Jaeger, J.C., Conduction of Heat in Solids, Second Edition, Clarendon Press, Oxford, 1959.

[10]Lamb, H., Hydrodynamics, Sixth Edition, Dover Publications, New York.

[11]White, F.M., *Viscous Fluid Flow,* McGraw-Hill, 1974.

[12]Riahi, D.N., *Flow Instability*, WIT Press, 2000.

[13]Prudnikov, A.P., Brychkov, Y.A., and Marichev, O.I., (Queen, N.M., Trans.), Integrals and Series, Volume 1: Elementary Functions, Gordon and Breach Science Publishers, New York, 1988.

[14]Gradshteyn, I.S., Ryzhik, I.M., (and Jeffrey, A., Ed.), Table of Integrals, Series, and Products, 5th Edition, Academic Press, Inc., San Diego, CA, 1994.

[15]Stanisic, M.M., The Mathematical Theory of Turbulence, Springer-Verlag, 1998.

[16]Han, Y.O., Leishman, J.G., and Coyne, A.J., "Measurements of the Velocity and Turbulence Structure of a Rotor Tip Vortex," AIAA Journal, Vol. 35, No. 3, March 1997.

[17]Ramasamy, M., Leishman, J.G., and Johnson, B., "Procedures for Measuring the Turbulence Characteristics of Rotor Blade Tip Vortices," AHS Specialist's Conference on Aeromechanics, San Francisco, CA, Jan. 23-25, 2008.

[18]Phillips, W.R.C. and Graham, J.A.H., "Reynolds-Stress Measurements in a Turbulent Trailing Vortex," J. Fluid Mech., Vol. 147, 1984, pp. 353-371.

[19]McAlister, K.W., and Heineck, J.T., "Measurements of the Early Development of Trailing Vorticity from a Rotor," NASA TP-2002-211848/AFDD TR-02-A-001, July 2002.

[20]Squire, H.B., "The Growth of a Vortex in Turbulent Flow," Aeronautical Quarterly, Vol. 16, Aug. 1965, pp. 302-306.

[21]Iversen, J.D., "Correlation of Turbulent Trailing Vortex Decay Data," Journal of Aircraft, Vol. 13, No. 5, May 1976, pp. 338-342.

[22]Hoffmann, E.R. and Joubert, P.N., "Turbulent Line Vortices," J. Fluid Mech., Vol. 16, 1963, pp. 395-411.

[23]Ramasamy, M. and Leishman, J.G., "Reynolds Number Based Blade Tip Vortex Model," 61st Annual Forum of the AHS International, Grapevine, TX, June 1-3, 2005.

[24]Govindaraju, S.P. and Saffman, P.G., "Flow in a Turbulent Trailing Vortex," Physics of Fluids, Vol. 14, 1971, pp. 2074-2080.

[25]Takahashi, R.K. and McAlister, K.W., "Preliminary Study of a Wing-Tip Vortex Using Laser Velocimetry," NASA TM 88343 , U.S. Army AVSCOM TM 86-A-2, January 1987.

[26]Beninati, M.L. and Marshall, J.S., "An Experimental Study of the Effect of Free-Stream Turbulence on a Trailing Vortex," Experiments in Fluids, Vol. 38, 2005, pp. 244-257.

[27]Abramowitz, M. and Stegun, I.A., *Handbook of Mathematical Functions with Formulas, Graphs, and Mathematical Tables*, AMS 55, U.S. Department of Commerce, November 1967.

[28]Fabre, D., Sipp, D., and Jacquin, L., "Kelvin Waves and the Singular Modes of the Lamb-Oseen Vortex," J. Fluid Mech., Vol. 551, 2006, pp. 235-274.

Appendix A – Analytical Treatment of Turbulent Flow

Consider the Helmholtz vorticity transport equation

$$\frac{D\boldsymbol{\omega}}{Dt} = (\boldsymbol{\omega}\cdot\nabla)\mathbf{V} + \nu\nabla^2\boldsymbol{\omega}$$

Which expands out to the form

$$\frac{\partial\omega_z}{\partial t} + v_r\frac{\partial\omega_z}{\partial r} + \frac{v_\theta}{r}\frac{\partial\omega_z}{\partial\theta} + v_z\frac{\partial\omega_z}{\partial z} =$$
$$\omega_r\frac{\partial v_z}{\partial r} + \frac{\omega_\theta}{r}\frac{\partial v_z}{\partial\theta} + \omega_z\frac{\partial v_z}{\partial z} + \nu\left\{\frac{\partial^2\omega_z}{\partial r^2} + \frac{1}{r}\frac{\partial\omega_z}{\partial r} + \frac{1}{r^2}\frac{\partial^2\omega_z}{\partial\theta^2} + \frac{\partial^2\omega_z}{\partial z^2}\right\}$$

$$\frac{\partial\omega_r}{\partial t} + v_r\frac{\partial\omega_r}{\partial r} + \frac{v_\theta}{r}\frac{\partial\omega_r}{\partial\theta} + v_z\frac{\partial\omega_r}{\partial z} =$$
$$\omega_r\frac{\partial v_r}{\partial r} + \frac{\omega_\theta}{r}\frac{\partial v_r}{\partial\theta} + \omega_z\frac{\partial v_r}{\partial z} + \nu\left\{\frac{\partial^2\omega_r}{\partial r^2} + \frac{1}{r}\frac{\partial\omega_r}{\partial r} + \frac{1}{r^2}\frac{\partial^2\omega_r}{\partial\theta^2} + \frac{\partial^2\omega_r}{\partial z^2}\right\}$$

$$\frac{\partial\omega_\theta}{\partial t} + v_r\frac{\partial\omega_\theta}{\partial r} + \frac{v_\theta}{r}\frac{\partial\omega_\theta}{\partial\theta} + v_z\frac{\partial\omega_\theta}{\partial z} =$$
$$\omega_r\frac{\partial v_\theta}{\partial r} + \frac{\omega_\theta}{r}\frac{\partial v_\theta}{\partial\theta} + \omega_z\frac{\partial v_\theta}{\partial z} + \nu\left\{\frac{\partial^2\omega_\theta}{\partial r^2} + \frac{1}{r}\frac{\partial\omega_\theta}{\partial r} + \frac{1}{r^2}\frac{\partial^2\omega_\theta}{\partial\theta^2} + \frac{\partial^2\omega_\theta}{\partial z^2}\right\}$$

(5a-d)

From previous work, Refs. 4-5, exact unsteady laminar flow solutions for a family of columnar vortices has been derived. This solution is summarized in Appendix B. This laminar flow solution is the basic flow state for the following detailed turbulent flow solution. For columnar/line vortices the mean flow state, by definition, requires only the axial vorticity and tangential velocities to be nonzero and that, correspondingly, $v_r = \omega_r = v_z = \omega_\theta = 0$.

Nondimensionalizing Eq. 5a-d yields the following[**]

$$v_r^\bullet\frac{\partial\omega_z^\bullet}{\partial r^\bullet} + \frac{v_\theta^\bullet}{r^\bullet}\frac{\partial\omega_z^\bullet}{\partial\theta} + v_z^\bullet\frac{\partial\omega_z^\bullet}{\partial z} =$$
$$\omega_r^\bullet\frac{\partial v_z^\bullet}{\partial r^\bullet} + \frac{\omega_\theta^\bullet}{r^\bullet}\frac{\partial v_z^\bullet}{\partial\theta} + \omega_z^\bullet\frac{\partial v_z^\bullet}{\partial z^\bullet} + \frac{1}{\mathrm{Re}}\left\{\frac{\partial^2\omega_z^\bullet}{\partial\left(r^\bullet\right)^2} + \frac{1}{r^\bullet}\frac{\partial\omega_z^\bullet}{\partial r^\bullet} + \frac{1}{\left(r^\bullet\right)^2}\frac{\partial^2\omega_z^\bullet}{\partial\theta^2} + \frac{\partial^2\omega_z^\bullet}{\partial\left(z^\bullet\right)^2} - \frac{\partial\omega_z^\bullet}{\partial t^\bullet}\right\}$$

[**] The θ–symmetry assumption only needs to be made (later) for this particular flow problem for the basic/mean flow and not the turbulent fluctuation velocities.

$$v_r^{\bullet}\frac{\partial \omega_r^{\bullet}}{\partial r^{\bullet}}+\frac{v_\theta^{\bullet}}{r^{\bullet}}\frac{\partial \omega_r^{\bullet}}{\partial \theta}+v_z^{\bullet}\frac{\partial \omega_r^{\bullet}}{\partial z^{\bullet}}=$$

$$\omega_r^{\bullet}\frac{\partial v_r^{\bullet}}{\partial r^{\bullet}}+\frac{\omega_\theta^{\bullet}}{r^{\bullet}}\frac{\partial v_r^{\bullet}}{\partial \theta}+\omega_z^{\bullet}\frac{\partial v_r^{\bullet}}{\partial z^{\bullet}}+\frac{1}{\mathrm{Re}}\left\{\frac{\partial^2 \omega_r^{\bullet}}{\partial\left(r^{\bullet}\right)^2}+\frac{1}{r^{\bullet}}\frac{\partial \omega_r^{\bullet}}{\partial r^{\bullet}}+\frac{1}{\left(r^{\bullet}\right)^2}\frac{\partial^2 \omega_r^{\bullet}}{\partial \theta^2}+\frac{\partial^2 \omega_r^{\bullet}}{\partial\left(z^{\bullet}\right)^2}-\frac{\partial \omega_r^{\bullet}}{\partial t^{\bullet}}\right\}$$

$$v_r^{\bullet}\frac{\partial \omega_\theta^{\bullet}}{\partial r^{\bullet}}+\frac{v_\theta^{\bullet}}{r^{\bullet}}\frac{\partial \omega_\theta^{\bullet}}{\partial \theta}+v_z^{\bullet}\frac{\partial \omega_\theta^{\bullet}}{\partial z^{\bullet}}=$$

$$\omega_r^{\bullet}\frac{\partial v_\theta^{\bullet}}{\partial r^{\bullet}}+\frac{\omega_\theta^{\bullet}}{r^{\bullet}}\frac{\partial v_\theta^{\bullet}}{\partial \theta}+\omega_z^{\bullet}\frac{\partial v_\theta^{\bullet}}{\partial z^{\bullet}}+\frac{1}{\mathrm{Re}}\left\{\frac{\partial^2 \omega_\theta^{\bullet}}{\partial\left(r^{\bullet}\right)^2}+\frac{1}{r^{\bullet}}\frac{\partial \omega_\theta^{\bullet}}{\partial r^{\bullet}}+\frac{1}{\left(r^{\bullet}\right)^2}\frac{\partial^2 \omega_\theta^{\bullet}}{\partial \theta^2}+\frac{\partial^2 \omega_\theta^{\bullet}}{\partial\left(z^{\bullet}\right)^2}-\frac{\partial \omega_\theta^{\bullet}}{\partial t^{\bullet}}\right\}$$

(6a-c)

Making, as noted in Refs. 4-5, the large Reynolds number assumption, Eq. 6a-c reduces to

$$v_r^{\bullet}\frac{\partial \omega_z^{\bullet}}{\partial r^{\bullet}}+\frac{v_\theta^{\bullet}}{r^{\bullet}}\frac{\partial \omega_z^{\bullet}}{\partial \theta}+v_z^{\bullet}\frac{\partial \omega_z^{\bullet}}{\partial z}=\omega_r^{\bullet}\frac{\partial v_z^{\bullet}}{\partial r^{\bullet}}+\frac{\omega_\theta^{\bullet}}{r^{\bullet}}\frac{\partial v_z^{\bullet}}{\partial \theta}+\omega_z^{\bullet}\frac{\partial v_z^{\bullet}}{\partial z^{\bullet}}$$

$$v_r^{\bullet}\frac{\partial \omega_r^{\bullet}}{\partial r^{\bullet}}+\frac{v_\theta^{\bullet}}{r^{\bullet}}\frac{\partial \omega_r^{\bullet}}{\partial \theta}+v_z^{\bullet}\frac{\partial \omega_r^{\bullet}}{\partial z^{\bullet}}=\omega_r^{\bullet}\frac{\partial v_r^{\bullet}}{\partial r^{\bullet}}+\frac{\omega_\theta^{\bullet}}{r^{\bullet}}\frac{\partial v_r^{\bullet}}{\partial \theta}+\omega_z^{\bullet}\frac{\partial v_r^{\bullet}}{\partial z^{\bullet}}$$

$$v_r^{\bullet}\frac{\partial \omega_\theta^{\bullet}}{\partial r^{\bullet}}+\frac{v_\theta^{\bullet}}{r^{\bullet}}\frac{\partial \omega_\theta^{\bullet}}{\partial \theta}+v_z^{\bullet}\frac{\partial \omega_\theta^{\bullet}}{\partial z^{\bullet}}\approx\omega_r^{\bullet}\frac{\partial v_\theta^{\bullet}}{\partial r^{\bullet}}+\frac{\omega_\theta^{\bullet}}{r^{\bullet}}\frac{\partial v_\theta^{\bullet}}{\partial \theta}+\omega_z^{\bullet}\frac{\partial v_\theta^{\bullet}}{\partial z^{\bullet}}$$

(7a-c)

Unlike the classic turbulent flow approach taken with Navier-Stokes Reynolds-averaging, e.g. Ref. 11, the velocity will be expressed as follows in terms of both a mean flow solution (defined in terms of the v_r, v_θ, and v_z velocity components) and "turbulent fluctuation" velocity components by $\hat{v}_r$, $\hat{v}_\theta$, and $\hat{v}_z$ (this alternate approach being more inspired, instead, by the classic treatment for fluid flow stability theory, e.g. Refs. 11-12, for "disturbance" velocities). At $t = 0$ the mean flow state is equivalent to the unsteady laminar flow solution summarized in Appendix B. The flow velocities can, therefore, be expressed as

$$\mathbf{V} = \begin{bmatrix} v_r + \hat{v}_r & v_\theta + \hat{v}_\theta & v_z + \hat{v}_z \end{bmatrix} \qquad (8)$$

In turn, this also implies (principally as a consequence of the length-scale factor methodology relating the axial and radial vorticity to the axial and radial velocity components) that the vorticity can be similarly expressed in terms of both a laminar, but unsteady, basic flow solution and turbulent fluctuation vorticity components.

$$\boldsymbol{\omega} = \begin{bmatrix} \omega_r + \hat{\omega}_r & \omega_\theta + \hat{\omega}_\theta & \omega_z + \hat{\omega}_z \end{bmatrix} \qquad (9)$$

Further, the mean flow state will be decomposed into laminar and turbulent components by means of the following expression

$$v_\theta = v_{\theta_L} + \Delta v_{\theta_T}$$

$$\omega_z = \omega_{z_L} + \Delta\omega_{z_T}$$

(10a-b)

The two flow components/solutions would be considered "superposed." Derivation of the laminar (basic) mean flow component is summarized in Appendix B. The turbulent mean flow component will be derived after, and indeed from, the turbulent fluctuation analytical expressions, at the close of this appendix.

Substitution of the above turbulent fluctuation expressions for the vorticity into the Helmholtz equations gives

$$\left(v_r^\bullet + \hat{v}_r^\bullet\right)\left(\frac{\partial\omega_z^\bullet}{\partial r^\bullet} + \frac{\partial\hat{\omega}_z^\bullet}{\partial r^\bullet}\right) + \frac{1}{r^\bullet}\left(v_\theta^\bullet + \hat{v}_\theta^\bullet\right)\left(\frac{\partial\omega_z^\bullet}{\partial\theta} + \frac{\partial\hat{\omega}_z^\bullet}{\partial\theta}\right) + \left(v_z^\bullet + \hat{v}_z^\bullet\right)\left(\frac{\partial\omega_z^\bullet}{\partial z} + \frac{\partial\hat{\omega}_z^\bullet}{\partial z}\right)$$
$$= \left(\omega_r^\bullet + \hat{\omega}_r^\bullet\right)\left(\frac{\partial v_z^\bullet}{\partial r^\bullet} + \frac{\partial\hat{v}_z^\bullet}{\partial r^\bullet}\right) + \frac{1}{r^\bullet}\left(\omega_\theta^\bullet + \hat{\omega}_\theta^\bullet\right)\left(\frac{\partial v_z^\bullet}{\partial\theta} + \frac{\partial\hat{v}_z^\bullet}{\partial\theta}\right) + \left(\omega_z^\bullet + \hat{\omega}_z^\bullet\right)\left(\frac{\partial v_z^\bullet}{\partial z^\bullet} + \frac{\partial\hat{v}_z^\bullet}{\partial z^\bullet}\right)$$

$$\left(v_r^\bullet + \hat{v}_r^\bullet\right)\left(\frac{\partial\omega_r^\bullet}{\partial r^\bullet} + \frac{\partial\hat{\omega}_r^\bullet}{\partial r^\bullet}\right) + \frac{1}{r^\bullet}\left(v_\theta^\bullet + \hat{v}_\theta^\bullet\right)\left(\frac{\partial\omega_r^\bullet}{\partial\theta} + \frac{\partial\hat{\omega}_r^\bullet}{\partial\theta}\right) + \left(v_z^\bullet + \hat{v}_z^\bullet\right)\left(\frac{\partial\omega_r^\bullet}{\partial z^\bullet} + \frac{\partial\hat{\omega}_r^\bullet}{\partial z^\bullet}\right)$$
$$= \left(\omega_r^\bullet + \hat{\omega}_r^\bullet\right)\left(\frac{\partial v_r^\bullet}{\partial r^\bullet} + \frac{\partial\hat{v}_r^\bullet}{\partial r^\bullet}\right) + \frac{1}{r^\bullet}\left(\omega_\theta^\bullet + \hat{\omega}_\theta^\bullet\right)\left(\frac{\partial v_r^\bullet}{\partial\theta} + \frac{\partial\hat{v}_r^\bullet}{\partial\theta}\right) + \left(\omega_z^\bullet + \hat{\omega}_z^\bullet\right)\left(\frac{\partial v_r^\bullet}{\partial z^\bullet} + \frac{\partial\hat{v}_r^\bullet}{\partial z^\bullet}\right)$$

$$\left(v_r^\bullet + \hat{v}_r^\bullet\right)\left(\frac{\partial\omega_\theta^\bullet}{\partial r^\bullet} + \frac{\partial\hat{\omega}_\theta^\bullet}{\partial r^\bullet}\right) + \frac{1}{r^\bullet}\left(v_\theta^\bullet + \hat{v}_\theta^\bullet\right)\left(\frac{\partial\omega_\theta^\bullet}{\partial\theta} + \frac{\partial\hat{\omega}_\theta^\bullet}{\partial\theta}\right) + \left(v_z^\bullet + \hat{v}_z^\bullet\right)\left(\frac{\partial\omega_\theta^\bullet}{\partial z^\bullet} + \frac{\partial\hat{\omega}_\theta^\bullet}{\partial z^\bullet}\right)$$
$$= \left(\omega_r^\bullet + \hat{\omega}_r^\bullet\right)\left(\frac{\partial v_\theta^\bullet}{\partial r^\bullet} + \frac{\partial\hat{v}_\theta^\bullet}{\partial r^\bullet}\right) + \frac{1}{r^\bullet}\left(\omega_\theta^\bullet + \hat{\omega}_\theta^\bullet\right)\left(\frac{\partial v_\theta^\bullet}{\partial\theta} + \frac{\partial\hat{v}_\theta^\bullet}{\partial\theta}\right) + \left(\omega_z^\bullet + \hat{\omega}_z^\bullet\right)\left(\frac{\partial v_\theta^\bullet}{\partial z^\bullet} + \frac{\partial\hat{v}_\theta^\bullet}{\partial z^\bullet}\right)$$

(11a-c)

Apply the θ–symmetry assumption to the mean flow portion of the equation and, further, assuming that either $v_r^\bullet = \omega_r^\bullet = v_z^\bullet = \omega_\theta^\bullet = 0$ or, as a minimum, $v_r^\bullet << \left|\hat{v}_r^\bullet\right|$, $v_z^\bullet << \left|\hat{v}_z^\bullet\right|$, $\omega_r^\bullet << \left|\hat{\omega}_r^\bullet\right|$, and $\omega_\theta^\bullet << \left|\hat{\omega}_\theta^\bullet\right|$. In other words, as a minimum the identified mean flow components are significantly smaller in magnitude than the absolute- or RMS-values (root-mean-square values) of the turbulent fluctuations of those same vorticity/velocity components. Accordingly, the mean flow components, $v_r^\bullet$, $v_z^\bullet$, $\omega_r^\bullet$, and $\omega_\theta^\bullet$, are assumed negligible in Eq. 11a-c. The turbulent fluctuations are, however, fully three-dimensional and of non-negligible magnitude.

$$\hat{v}_r^\bullet\left(\frac{\partial\omega_z^\bullet}{\partial r^\bullet} + \frac{\partial\hat{\omega}_z^\bullet}{\partial r^\bullet}\right) + \frac{1}{r^\bullet}\left(v_\theta^\bullet + \hat{v}_\theta^\bullet\right)\frac{\partial\hat{\omega}_z^\bullet}{\partial\theta} + \hat{v}_z^\bullet\frac{\partial\hat{\omega}_z^\bullet}{\partial z}$$
$$= \hat{\omega}_r^\bullet\frac{\partial\hat{v}_z^\bullet}{\partial r^\bullet} + \frac{\hat{\omega}_\theta^\bullet}{r^\bullet}\frac{\partial\hat{v}_z^\bullet}{\partial\theta} + \left(\omega_z^\bullet + \hat{\omega}_z^\bullet\right)\frac{\partial\hat{v}_z^\bullet}{\partial z^\bullet}$$

$$\hat{v}_r^\bullet\frac{\partial\hat{\omega}_r^\bullet}{\partial r^\bullet} + \frac{1}{r^\bullet}\left(v_\theta^\bullet + \hat{v}_\theta^\bullet\right)\frac{\partial\hat{\omega}_r^\bullet}{\partial\theta} + \hat{v}_z^\bullet\frac{\partial\hat{\omega}_r^\bullet}{\partial z^\bullet}$$
$$= \hat{\omega}_r^\bullet\frac{\partial\hat{v}_r^\bullet}{\partial r^\bullet} + \frac{\hat{\omega}_\theta^\bullet}{r^\bullet}\frac{\partial\hat{v}_r^\bullet}{\partial\theta} + \left(\omega_z^\bullet + \hat{\omega}_z^\bullet\right)\frac{\partial\hat{v}_r^\bullet}{\partial z^\bullet}$$

$$\hat{v}_r^{\bullet}\frac{\partial\hat{\omega}_\theta^{\bullet}}{\partial r^{\bullet}}+\frac{1}{r^{\bullet}}\left(v_\theta^{\bullet}+\hat{v}_\theta^{\bullet}\right)\frac{\partial\hat{\omega}_\theta^{\bullet}}{\partial\theta}+\hat{v}_z^{\bullet}\frac{\partial\hat{\omega}_\theta^{\bullet}}{\partial z^{\bullet}}$$
$$=\hat{\omega}_r^{\bullet}\left(\frac{\partial v_\theta^{\bullet}}{\partial r^{\bullet}}+\frac{\partial\hat{v}_\theta^{\bullet}}{\partial r^{\bullet}}\right)+\frac{1}{r^{\bullet}}\hat{\omega}_\theta^{\bullet}\frac{\partial\hat{v}_\theta^{\bullet}}{\partial\theta}+\left(\omega_z^{\bullet}+\hat{\omega}_z^{\bullet}\right)\frac{\partial\hat{v}_\theta^{\bullet}}{\partial z^{\bullet}}$$

(12a-c)

Applying length scale factor assumptions to the turbulent fluctuation velocities (Refs. 4-7) yields

$$\hat{v}_z\approx-\ell\hat{\omega}_z$$
$$\hat{v}_r\approx-\ell\hat{\omega}_r$$
$$\hat{v}_\theta\approx-\ell\hat{\omega}_\theta$$

(13a-c)

Note the following nondimensionalization of the length scale factor: $\ell^{\bullet}=\ell/r_{c0}$.

Unlike the previous work of Refs. 4-5, the length scale factor, ℓ, is applied throughout the whole flow field and not discretely applied to partitioned regions of flow separated by wave-front boundaries.[††] Accordingly,

$$\ell=-r_{c0}\qquad\text{And}\qquad\ell^{\bullet}=-1$$

(14a-b)

Making the above substitutions yields

$$\hat{v}_r^{\bullet}\left(\frac{\partial\omega_z^{\bullet}}{\partial r^{\bullet}}+\frac{\partial\hat{\omega}_z^{\bullet}}{\partial r^{\bullet}}\right)+\frac{1}{r^{\bullet}}\left(v_\theta^{\bullet}+\hat{v}_\theta^{\bullet}\right)\frac{\partial\hat{\omega}_z^{\bullet}}{\partial\theta}+\hat{v}_z^{\bullet}\frac{\partial\hat{\omega}_z^{\bullet}}{\partial z^{\bullet}}=\hat{\omega}_r^{\bullet}\frac{\partial\hat{v}_z^{\bullet}}{\partial r^{\bullet}}+\frac{\hat{\omega}_\theta^{\bullet}}{r^{\bullet}}\frac{\partial\hat{v}_z^{\bullet}}{\partial\theta}+\left(\omega_z^{\bullet}+\hat{\omega}_z^{\bullet}\right)\frac{\partial\hat{v}_z^{\bullet}}{\partial z^{\bullet}}$$
$$\downarrow$$
$$\ell^{\bullet}\frac{\partial\omega_z^{\bullet}}{\partial r^{\bullet}}\hat{v}_r^{\bullet}-\frac{v_\theta^{\bullet}}{r^{\bullet}}\frac{\partial\hat{v}_z^{\bullet}}{\partial\theta}-\ell^{\bullet}\omega_z^{\bullet}\frac{\partial\hat{v}_z^{\bullet}}{\partial z^{\bullet}}=0$$

$$\hat{v}_r^{\bullet}\frac{\partial\hat{\omega}_r^{\bullet}}{\partial r^{\bullet}}+\frac{1}{r^{\bullet}}\left(v_\theta^{\bullet}+\hat{v}_\theta^{\bullet}\right)\frac{\partial\hat{\omega}_r^{\bullet}}{\partial\theta}+\hat{v}_z^{\bullet}\frac{\partial\hat{\omega}_r^{\bullet}}{\partial z^{\bullet}}=\hat{\omega}_r^{\bullet}\frac{\partial\hat{v}_r^{\bullet}}{\partial r^{\bullet}}+\frac{\hat{\omega}_\theta^{\bullet}}{r^{\bullet}}\frac{\partial\hat{v}_r^{\bullet}}{\partial\theta}+\left(\omega_z^{\bullet}+\hat{\omega}_z^{\bullet}\right)\frac{\partial\hat{v}_r^{\bullet}}{\partial z^{\bullet}}$$
$$\downarrow$$
$$\frac{v_\theta^{\bullet}}{r^{\bullet}}\frac{\partial\hat{v}_r^{\bullet}}{\partial\theta}+\ell^{\bullet}\omega_z^{\bullet}\frac{\partial\hat{v}_r^{\bullet}}{\partial z^{\bullet}}=0$$

$$\hat{v}_r^{\bullet}\frac{\partial\hat{\omega}_\theta^{\bullet}}{\partial r^{\bullet}}+\frac{1}{r^{\bullet}}\left(v_\theta^{\bullet}+\hat{v}_\theta^{\bullet}\right)\frac{\partial\hat{\omega}_\theta^{\bullet}}{\partial\theta}+\hat{v}_z^{\bullet}\frac{\partial\hat{\omega}_\theta^{\bullet}}{\partial z^{\bullet}}=\hat{\omega}_r^{\bullet}\left(\frac{\partial v_\theta^{\bullet}}{\partial r^{\bullet}}+\frac{\partial\hat{v}_\theta^{\bullet}}{\partial r^{\bullet}}\right)+\frac{1}{r^{\bullet}}\hat{\omega}_\theta^{\bullet}\frac{\partial\hat{v}_\theta^{\bullet}}{\partial\theta}+\left(\omega_z^{\bullet}+\hat{\omega}_z^{\bullet}\right)\frac{\partial\hat{v}_\theta^{\bullet}}{\partial z^{\bullet}}$$
$$\downarrow$$
$$\frac{v_\theta^{\bullet}}{r^{\bullet}}\frac{\partial\hat{v}_\theta^{\bullet}}{\partial\theta}-\hat{v}_r^{\bullet}\frac{\partial v_\theta^{\bullet}}{\partial r^{\bullet}}+\ell^{\bullet}\omega_z^{\bullet}\frac{\partial\hat{v}_\theta^{\bullet}}{\partial z^{\bullet}}=0$$

(15a-c)

[††] This may be a matter of subtle interpretation, in this particular case. Later in this paper, in deriving a function for the radial distribution of the radial and tangential turbulence, i.e. $g\left(r,t^{\bullet}\right)$, a "cutoff" parameter α is introduced, with an associated "smoothing" function, for the turbulence centered at a discrete radial boundary. Within this boundary the flow is turbulent; outside this boundary the turbulence rapidly drops off. This boundary, associated with the cutoff parameter α, is a function of time and, therefore, could in fact be interpreted as a propagating wave-front boundary similar to those employed/identified in the above noted earlier work, Refs. 4-5.

The mean flow vorticity and velocities will be determined later in the paper, but for the following discussion regarding derivation of the turbulent fluctuation solutions, the mean flow components are assumed already known. Note, though, for small values of time, the mean flow values of $\omega_z^\bullet$ and $v_\theta^\bullet$ are approximately equal to the values predicted by the unsteady laminar solution summarized in Appendix B.

Equation 15b can be solved by the method of separation of variables for the radial turbulent fluctuation velocity. Letting $A = \ell^\bullet r^\bullet \omega_z^\bullet / v_\theta^\bullet$ and $\hat{v}_r^\bullet = h_0(\theta)\zeta_0\left(z^\bullet\right)$, Eq. 15b becomes

$$\frac{1}{h_0}\frac{\partial h_0}{\partial \theta} + \frac{A}{\zeta_0}\frac{\partial \zeta_0}{\partial z^\bullet} = 0 \tag{16}$$

The above is separable into two equations

$$\frac{1}{h_0}\frac{\partial h_0}{\partial \theta} = b$$

$$\frac{A}{\zeta_0}\frac{\partial \zeta_0}{\partial z^\bullet} = -b \tag{17a-b}$$

The elemental solutions of the above two equations, $h_0(\theta) = \alpha e^{b\theta}$ and $\zeta_0\left(z^\bullet\right) = e^{-bz^\bullet/A}$, gives the result $\hat{v}_r^\bullet \propto \alpha e^{b\left(\theta - z^\bullet/A\right)}$, where α is an arbitrary constant with respect to θ and $z^\bullet$. However, because Eq. 17a-b are linear first order ordinary differential equations, and because the solution has to be periodic with respect to θ and $z^\bullet$, the complete solution of Eq. 15b must be represented by the superposition of elemental solution such that

$$\hat{v}_r^\bullet \propto \alpha_1 e^{b_1\left(\theta - z^\bullet/A\right)} + \alpha_2 e^{b_2\left(\theta - z^\bullet/A\right)} \tag{18}$$

Letting $\alpha_2 = -\alpha_1 = -f_m^*\left(r^\bullet, t^\bullet\right)/2i$, $b_1 = mi$, $b_2 = -mi$, and applying the Euler's equation and derivative expressions relating complex exponential functions to trigonometric functions, specifically $\sin x = \left(e^{ix} - e^{-ix}\right)/2i$, yields

$$\hat{v}_r^\bullet \propto f_m^\bullet\left(r^\bullet, t^\bullet\right)\sin\left(m\left(\theta - z^\bullet/A\right)\right) \tag{19}$$

In general, therefore, the problem can be satisfied by an expression of the following form

$$\hat{v}_r^\bullet = C_1 + \sum_{m=1}^{\infty^-} f_m^*\left(r^\bullet, t^\bullet\right)\sin\left(m\left(\theta - z^\bullet/A\right) + \varphi_m^*\left(r^\bullet, t^\bullet\right)\right)$$

Where, again

$$A = \ell^\bullet r^\bullet \omega_z^\bullet / v_\theta^\bullet \tag{20a-b}$$

And C_1 is a constant with respect to $z^\bullet$ and θ, but otherwise could be a function with respect to $r^\bullet$ and $t^\bullet$. The constant C_1 could represent an external and/or background turbulence field in which the vortex is

embedded. For the purposes of this analysis it can be assumed with a negligible loss of generality that $C_1 = 0$. Requiring that $f_m^*\left(r^\bullet, t^\bullet\right)$ be quasi-separable in the sense that

$$f_m^*\left(r^\bullet, t^\bullet\right) = g(r,t) f_m\left(t^\bullet\right)$$

Where

$$\frac{\partial}{\partial t^\bullet} g\left(r^\bullet, t^\bullet\right) << \frac{\partial}{\partial t^\bullet} f_m\left(t^\bullet\right) \tag{21a-b}$$

The solution for $\hat{v}_r^\bullet$ can then be recast as

$$\hat{v}_r^\bullet = g\left(r^\bullet, t^\bullet\right)\left\{\sum_{m=1}^{\infty^-} f_m\left(t^\bullet\right) \sin\left(m\left(\theta - z^\bullet / A\right) + \varphi_m\left(t^\bullet\right)\right)\right\} \tag{22}$$

Equation 22 implies that the instantaneous fluctuating radial velocity distribution will take on a helical distribution. The exact complexity of these helical structures will be dependent upon the order of modes, m, being considered in the analysis, as well as the exact form/functionality of the amplitude and phase functions, $f_m\left(t^\bullet\right)$ and $\varphi_m\left(t^\bullet\right)$. Note that at least as far as continuity and Eq. 15b are concerned, both $f_m\left(t^\bullet\right)$ and $\varphi_m\left(t^\bullet\right)$ can have both deterministic and stochastic contributions. This will be discussed in greater detail later in the paper. ‡‡

Next, Eq. 15c will be used to solve for the tangential velocity component, $\hat{v}_\theta^\bullet$. Using the previous definition $A = \ell^\bullet r^\bullet \omega_z^\bullet / v_\theta^\bullet$, Eq. 15c becomes

$$\frac{\partial \hat{v}_\theta^\bullet}{\partial \theta} + A \frac{\partial \hat{v}_\theta^\bullet}{\partial z^\bullet} + B \hat{v}_r^\bullet = 0$$

Where

$$B = -\frac{r^\bullet}{v_\theta^\bullet} \frac{\partial v_\theta^\bullet}{\partial r^\bullet} \tag{23a-b}$$

Assuming a separable solution for $\hat{v}_\theta^\bullet$ of the form $\hat{v}_\theta^\bullet = h_1(\theta)\xi_1\left(z^\bullet\right)$, then Eq. 23a becomes

---

‡‡ Verifying the $\hat{v}_r^\bullet$ solution, Eq. 22 is substituted back into Eq. 15b.

$$\frac{v_\theta^\bullet}{r^\bullet} \frac{\partial \hat{v}_r^\bullet}{\partial \theta} + \ell^\bullet \omega_z^\bullet \frac{\partial \hat{v}_r^\bullet}{\partial z^\bullet} = 0$$

$$\downarrow$$

$$\frac{\partial \hat{v}_r^\bullet}{\partial \theta} + A \frac{\partial \hat{v}_r^\bullet}{\partial z^\bullet} = 0$$

$$\downarrow$$

$$g\left(r^\bullet, t^\bullet\right)\left\{\sum_{m=1}^{\infty^-} m f_m\left(t^\bullet\right) \cos\left(m\left(\theta - \frac{z^\bullet}{A}\right) + \varphi_m\left(t^\bullet\right)\right)\right\} + (-1) A g\left(r^\bullet, t^\bullet\right)\left\{\sum_{m=1}^{\infty^-} \frac{m}{A} f_m\left(t^\bullet\right) \cos\left(m\left(\theta - \frac{z^\bullet}{A}\right) + \varphi_m\left(t^\bullet\right)\right)\right\} = 0$$

$$\downarrow$$

$$0 = 0$$

$$\frac{1}{h_1}\frac{\partial h_1}{\partial \theta}+\frac{A}{\zeta_1}\frac{\partial \zeta_1}{\partial z^\bullet}+B\frac{h_0\zeta_0}{h_1\zeta_1}=0 \tag{24}$$

Equation 24 can be partially separated as follows

$$\frac{A}{\zeta_1}\frac{\partial \zeta_1}{\partial z^\bullet}=-\beta$$

$$\frac{1}{h_1}\frac{\partial h_1}{\partial \theta}+B\frac{h_0\zeta_0}{h_1\zeta_1}=\beta \tag{25a-b}$$

Solving Eq. 25a for $\zeta_1\left(z^\bullet\right)$ gives $\zeta_1\left(z^\bullet\right)\propto e^{-\beta z^\bullet/A}$. Given this result, if it is assumed that $\beta=b$, then $\zeta_1\left(z^\bullet\right)=\zeta_0\left(z^\bullet\right)$. The consequence of this second result is that Eq. 25a-b is now fully separable and Eq. 25b becomes

$$\frac{\partial h_1}{\partial \theta}-\beta h_1+Bh_0=0 \tag{26}$$

This first-order ordinary differential equation can be straightforwardly solved for. The result is

$$\begin{aligned} h_1 &= e^{\int \beta d\theta}\left\{\kappa - B\int h_0(\theta)e^{-\int \beta d\theta}d\theta\right\}=e^{b\theta}\left\{\kappa - B\int h_0(\theta)e^{-b\theta}d\theta\right\} \\ &= e^{b\theta}\left\{\kappa - B\int \alpha d\theta\right\}=(\kappa-\alpha B\theta)e^{b\theta} \end{aligned} \tag{27}$$

The complete solution for $\hat{v}_\theta^\bullet$ has to be quasi-periodic and, therefore, given the linearity of the equations involved, superposition can be employed. Further, using complex exponential functions gives

$$\hat{v}_\theta^\bullet \propto (\kappa_1-\alpha_1 B\theta)e^{b_1\left(\theta-z^\bullet/A\right)}+(\kappa_2-\alpha_2 B\theta)e^{b_2\left(\theta-z^\bullet/A\right)} \tag{28}$$

Where, as before, $\alpha_1=-\alpha_2=f_m^*\left(r^\bullet,t^\bullet\right)\big/2i$, $b_1=mi$, and $b_2=-mi$. New arbitrary constants, with respect to θ and $z^\bullet$, are introduced where $\kappa_1=-\kappa_2=g_m^*\left(r^\bullet,t^\bullet\right)\big/2i$.

The general solution for $\hat{v}_\theta^\bullet$ is consequently given by the expression

$$\hat{v}_\theta^\bullet = C_2+\sum_{m=1}^{\infty^-}\left(g_m^*\left(r^\bullet,t^\bullet\right)-f_m^*\left(r^\bullet,t^\bullet\right)B\theta\right)\sin\left(m\left(\theta-z^\bullet/A\right)+\varphi_m^*\left(r^\bullet,t^\bullet\right)\right) \tag{29}$$

Where C_2 is again a constant with respect to $z^\bullet$ and θ, but otherwise is a function with respect to $r^\bullet$ and $t^\bullet$. Again, with negligible loss of generality, it is assumed that $C_2=0$. Equation 29 is only valid for the range $z^\bullet/A-\varphi_m^*\left(r^\bullet,t^\bullet\right)\big/m\le\theta\le 2\pi+z^\bullet/A-\varphi_m^*\left(r^\bullet,t^\bullet\right)\big/m$ and, further, limited to $-2\pi\le z^\bullet/A\le 2\pi$, where outside this axial coordinate range successive "mirroring" of the flow can be employed. Note

though that the "mirror" plane-of-symmetry axial locations, in terms of $z^{\bullet}$, are a function of the radial coordinate, $r^{\bullet}$, of the points being evaluated. Such required mirroring of the turbulent helical flow structures begins at a much larger axial location for points near the vortex centerline than it does for the outer regions of the vortex because $A \to 0$ as $r^{\bullet} >> 0$.

The solution for $\hat{v}_{\theta}^{\bullet}$ is assumed to be quasi-separable in the context of Eq. 21a-b. Next, the higher-mode time-dependent function, $f_m^*\left(r^{\bullet},t^{\bullet}\right)$, is decomposed/separated into two simpler functions $\chi(m)$ and $f\left(m,t^{\bullet}\right)$, such that $f_m\left(t^{\bullet}\right) = \chi(m) f\left(m,t^{\bullet}\right)$ where as previously prescribed $f_m^*\left(r^{\bullet},t^{\bullet}\right) = g\left(r^{\bullet},t^{\bullet}\right) f_m\left(t^{\bullet}\right)$. In turn, making the assumption that $g_m^*\left(r^{\bullet},t^{\bullet}\right) = g\left(r^{\bullet},t^{\bullet}\right)\beta\left(m,r^{\bullet},t^{\bullet}\right)$ where $\beta_m\left(r^{\bullet},t^{\bullet}\right) \equiv \chi(m)\left(\varepsilon\left(m,r^{\bullet},t^{\bullet}\right) + f\left(m,t^{\bullet}\right)\right)$, $\varepsilon\left(m,r^{\bullet},t^{\bullet}\right) \equiv \vartheta \cdot \max\left(f_m\left(t^{\bullet}\right)\right)\cdot(1+A)$, and ϑ is an arbitrary multiplier constant, i.e. the "offset" or "skew" of the tangential turbulent fluctuation. Note that $\max\left(f_m\left(t^{\bullet}\right)\right) \approx \max\left(f\left(1,t^{\bullet}\right)\right)$. Without this offset or skew there can be no net mean flow resulting from the tangential velocity turbulent fluctuation. It imposes an assumed radial distribution, the $(1+A)$ term in the $\varepsilon\left(m,r^{\bullet},t^{\bullet}\right)$ function, to the turbulent fluctuation skew. The assumed skew radial distribution has five important characteristics: (1) $\varepsilon\left(m,r^{\bullet},t^{\bullet}\right) \propto (1+A) \to 0$ as $r^{\bullet} \to 0$, (2) $\partial\varepsilon\left(m,r^{\bullet},t^{\bullet}\right)\Big/\partial r^{\bullet} \propto \partial(1+A)\big/\partial r^{\bullet} = \partial A\big/\partial r^{\bullet} \to 0$ as $r^{\bullet} \to 0$, (3) $\varepsilon\left(m,r^{\bullet},t^{\bullet}\right) \propto (1+A) \to 1$ as $r^{\bullet} \to \infty$, (4) $\partial\varepsilon\left(m,r^{\bullet},t^{\bullet}\right)\Big/\partial r^{\bullet} \propto \partial(1+A)\big/\partial r^{\bullet} = \partial A\big/\partial r^{\bullet} \to 0$ as $r^{\bullet} \to \infty$, and (5) the radial expanse to which A has non-zero values expands with time, in parallel with the vortex core radius growth. It is important to note that the $(1+A)$ term is of relatively low order; follow-on analyses refining the functionality of $\varepsilon\left(m,r^{\bullet},t^{\bullet}\right)$ might require higher-order terms. Proceeding, nonetheless, the above assumed functional relationships yields the expression

$$\hat{v}_{\theta}^{\bullet} = g\left(r^{\bullet},t^{\bullet}\right)\left\{\sum_{m=1}^{\infty^{-}}\left(\beta_m\left(r^{\bullet},t^{\bullet}\right) - f_m\left(t^{\bullet}\right)B\theta\right)\sin\left(m\left(\theta - z^{\bullet}/A\right) + \varphi_m\left(t^{\bullet}\right)\right)\right\} \tag{30}$$

The above functional decomposition will shortly be seen as being critical to addressing a number of anticipated analysis issues. The introduction of the quantity $\varepsilon\left(m,r^{\bullet},t^{\bullet}\right) + f\left(m,t^{\bullet}\right)$ in the $\beta_m\left(r^{\bullet},t^{\bullet}\right)$ function dictates that the tangential velocity fluctuations are skewed positive in sign by the offset quantity $\varepsilon\left(m,r^{\bullet},t^{\bullet}\right)$.[§§] The radial and axial turbulent fluctuation solutions do not have such offsets and, therefore,

---

[§§] By way of further exposition, if $f\left(m,t^{\bullet}\right)$ were described by a single undamped sinusoidal mode, say for example, $f\left(m,t^{\bullet}\right) = a\cdot\cos\left(mt^{\bullet}\right)$, then $\varepsilon\left(m,r^{\bullet},t^{\bullet}\right) = a\cdot(1+A)$ for a fully skewed positive fluctuation, i.e. $\vartheta = 1$. This skewing needs to be implemented so that, after time-averaging, the tangential fluctuation solution will yield a net nonzero turbulent mean flow distribution for the vortex. Using the previous simple example, without this skewing or offset, $\varepsilon\left(m,r^{\bullet},t^{\bullet}\right) = 0$, therefore, $(1/T)\int_t^{t+T} f(m,\tau)d\tau = (1/T)\int_t^{t+T} a\cdot\cos(m\tau)d\tau \to 0$. Alternatively, with skewing, $\varepsilon\left(m,r^{\bullet},t^{\bullet}\right) = a\cdot(1+A)$ and, consequently, $(1/T)\int_t^{t+T}\left(\varepsilon\left(m,r^{\bullet},t^{\bullet}\right) + f(m,\tau)\right)d\tau = (a/T)\int_t^{t+T}\left(1+A+\cos(m\tau)\right)d\tau$, or $(1/T)\int_t^{t+T}\left(\varepsilon\left(m,r^{\bullet},t^{\bullet}\right) + f(m,\tau)\right)d\tau \to a\cdot(1+A)$, and therefore a net mean flow radial distribution is introduced.

time-averaging of these solutions yields zero mean turbulent flow for these velocity components. This reinforces the proposed interpretation (Ref. 7) of transitional and fully-developed turbulent flow as being intermediate, and transitory, states between two extremes – the laminar basic flow state and a never-fully-realized meta-state. The role of the $\varepsilon\left(m,r^{\bullet},t^{\bullet}\right)$ offset will be clearly seen at the close of this appendix, during the derivation of the tangential velocity turbulent mean flow distribution. Note that the function $\beta_m\left(r^{\bullet},t^{\bullet}\right)$ is completely defined when $g\left(r^{\bullet},t^{\bullet}\right)$ and $f_m\left(t^{\bullet}\right)$ are defined. Finally, in the above solution for $\hat{v}_{\theta}^{\bullet}$, the requirement that $\hat{v}_{\theta}^{\bullet}\big|_{\theta=0} = \hat{v}_{\theta}^{\bullet}\big|_{\theta=2\pi}$ is automatically satisfied by employing the sine terms and limiting the range of applicability of Eq. 30 to $z^{\bullet}/A - \varphi_m^*\left(r^{\bullet},t^{\bullet}\right)\big/m \le \theta \le 2\pi + z^{\bullet}/A - \varphi_m^*\left(r^{\bullet},t^{\bullet}\right)\big/m$ and, again, limited to $-2\pi \le z^{\bullet}/A \le 2\pi$, as well.

Next, Eq. 15a will be considered for solving for $\hat{v}_z^{\bullet}$. The resultant form of Eq. 15a, employing the previously defined parameter A, is

$$\frac{\partial \hat{v}_z^{\bullet}}{\partial \theta} + A\frac{\partial \hat{v}_z^{\bullet}}{\partial z^{\bullet}} + C\hat{v}_r^{\bullet} = 0$$

Where

$$C = -\frac{\ell^{\bullet} r^{\bullet}}{v_{\theta}^{\bullet}}\frac{\partial \omega_z^{\bullet}}{\partial r^{\bullet}}$$

(31a-b)

Effectively the Eq. 31a first-order partial differential equation has the same functional form as Eq. 23a and consequently has the same general solution.*** Therefore, the general solution for $\hat{v}_z^{\bullet}$ is given by the expression

$$\hat{v}_z^{\bullet} = C_3 + \sum_{m=1}^{\infty^-}\left(h_m^*\left(r^{\bullet},t^{\bullet}\right) - f_m^*\left(r^{\bullet},t^{\bullet}\right)C\theta\right)\sin\left(m\left(\theta - z^{\bullet}/A\right) + \varphi_m^*\left(r^{\bullet},t^{\bullet}\right)\right)$$

(32)

*** Verifying the $\hat{v}_{\theta}^{\bullet}$ solution, Eq. 30 is substituted back into Eq. 15c.

$$\frac{\partial \hat{v}_{\theta}^{\bullet}}{\partial \theta} + A\frac{\partial \hat{v}_{\theta}^{\bullet}}{\partial z^{\bullet}} + B\hat{v}_r^{\bullet} = 0$$

$$\downarrow$$

$$g\left(r^{\bullet},t^{\bullet}\right)\left\{\sum_{m=1}^{\infty^-}\left(-Bf_m\left(t^{\bullet}\right)\right)\sin\left(m\left(\theta - z^{\bullet}/A\right) + \lambda_m\left(t^{\bullet}\right)\right)\right\} + g\left(r^{\bullet},t^{\bullet}\right)\left\{\sum_{m=1}^{\infty^-} m\left(\beta_m\left(r^{\bullet},t^{\bullet}\right) - f_m\left(t^{\bullet}\right)B\theta\right)\cos\left(m\left(\theta - z^{\bullet}/A\right) + \varphi_m\left(t^{\bullet}\right)\right)\right\}$$

$$+A\left(-\frac{1}{A}\right)g\left(r^{\bullet},t^{\bullet}\right)\left\{\sum_{m=1}^{\infty^-} m\left(\beta_m\left(r^{\bullet},t^{\bullet}\right) - f_m\left(t^{\bullet}\right)B\theta\right)\cos\left(m\left(\theta - z^{\bullet}/A\right) + \varphi_m\left(t^{\bullet}\right)\right)\right\} + Bg\left(r^{\bullet},t^{\bullet}\right)\left\{\sum_{m=1}^{\infty^-} f_m\left(t^{\bullet}\right)\cos\left(m\left(\theta - z^{\bullet}/A\right) + \varphi_m\left(t^{\bullet}\right)\right)\right\} = 0$$

$$\downarrow$$

$$g\left(r^{\bullet},t^{\bullet}\right)\left\{\sum_{m=1}^{\infty^-} m\left(\beta_m\left(r^{\bullet},t^{\bullet}\right) - f_m\left(t^{\bullet}\right)B\theta\right)\cos\left(m\left(\theta - z^{\bullet}/A\right) + \varphi_m\left(t^{\bullet}\right)\right)\right\} - g\left(r^{\bullet},t^{\bullet}\right)\left\{\sum_{m=1}^{\infty^-} m\left(\beta_m\left(r^{\bullet},t^{\bullet}\right) - f_m\left(t^{\bullet}\right)B\theta\right)\cos\left(m\left(\theta - z^{\bullet}/A\right) + \varphi_m\left(t^{\bullet}\right)\right)\right\} = 0$$

$$\downarrow$$

$$0 = 0$$

Note that the constant C_3 is assumed equal to zero without any significant loss of generality. And, correspondingly a quasi-separable version of the solution for $\hat{v}_z^\bullet$ can be defined by making the assumption that $h_m^*\left(r^\bullet,t^\bullet\right)=h\left(r^\bullet,t^\bullet\right)f_m\left(t^\bullet\right)$ and $f_m^*\left(r^\bullet,t^\bullet\right)=g\left(r^\bullet,t^\bullet\right)f_m\left(t^\bullet\right)$, but, further, unlike previously, in this case $\kappa\neq\alpha$ and, specifically $h\left(r^\bullet,t^\bullet\right)\neq g\left(r^\bullet,t^\bullet\right)$. This distinction -- for the radial functionality of $\hat{v}_r^\bullet\propto g\left(r^\bullet,t^\bullet\right)$ and $\hat{v}_\theta^\bullet\propto g\left(r^\bullet,t^\bullet\right)$ versus $\hat{v}_z^\bullet$ being a linear composite of the, as yet, undefined functions $g\left(r^\bullet,t^\bullet\right)$ and $h\left(r^\bullet,t^\bullet\right)$ -- is key to satisfying the continuity equation. Therefore, given this,

$$\hat{v}_z^\bullet=\sum_{m=1}^{\infty^-}f_m\left(t^\bullet\right)\left(h\left(r^\bullet,t^\bullet\right)-g\left(r^\bullet,t^\bullet\right)C\theta\right)\sin\left(m\left(\theta-z^\bullet/A\right)+\varphi_m\left(t^\bullet\right)\right) \tag{33}$$

The solutions for $\hat{v}_r^\bullet$, $\hat{v}_\theta^\bullet$, and $\hat{v}_z^\bullet$ are not yet complete as the functions defining both the radial coordinate and time dependence (amplitude and phase of each of the discrete modes) of these velocity components have not been derived.††† The next step in completing the overall solution is to explicitly consider the continuity equation. As the flow can no longer be considered axisymmetric, the full continuity equation is employed.

$$\begin{gathered}\frac{1}{r}\frac{\partial}{\partial r}\left(rv_r\right)+\frac{1}{r}\frac{\partial v_\theta}{\partial\theta}+\frac{\partial v_z}{\partial z}=0\\ \downarrow\\ \frac{1}{r^\bullet}\frac{\partial}{\partial r^\bullet}\left(r^\bullet\hat{v}_r^\bullet\right)+\frac{1}{r^\bullet}\frac{\partial\hat{v}_\theta^\bullet}{\partial\theta}+\frac{\partial\hat{v}_z^\bullet}{\partial z^\bullet}=0\end{gathered} \tag{34}$$

Next, making the applicable substitutions for the turbulent fluctuation velocity components to the continuity equation, gives

---

††† Verifying the $\hat{v}_z^\bullet$ solution, Eq. 32 is substituted back into Eq. 15a.

$$\frac{\partial\hat{v}_z^\bullet}{\partial\theta}+A\frac{\partial\hat{v}_z^\bullet}{\partial z^\bullet}+C\hat{v}_r^\bullet=0$$

$$\downarrow$$

$$-Cg\left(r^\bullet,t^\bullet\right)\sum_{m=1}^{\infty^-}f_m\left(t^\bullet\right)\sin\left(m\left(\theta-z^\bullet/A\right)+\varphi_m\left(t^\bullet\right)\right)-\sum_{m=1}^{\infty^-}mf_m\left(t^\bullet\right)\left(h\left(r^\bullet,t^\bullet\right)-g\left(r^\bullet,t^\bullet\right)C\theta\right)\cos\left(m\left(\theta-z^\bullet/A\right)+\varphi_m\left(t^\bullet\right)\right)$$

$$+(-1)A\sum_{m=1}^{\infty^-}\left(-\frac{m}{A}\right)f_m\left(t^\bullet\right)\left(h\left(r^\bullet,t^\bullet\right)-g\left(r^\bullet,t^\bullet\right)C\theta\right)\cos\left(m\left(\theta-z^\bullet/A\right)+\varphi_m\left(t^\bullet\right)\right)+C\left\{g\left(r^\bullet,t^\bullet\right)\left\{\sum_{m=1}^{\infty^-}f_m\left(t^\bullet\right)\sin\left(m\left(\theta-z^\bullet/A\right)+\varphi_m\left(t^\bullet\right)\right)\right\}\right\}=0$$

$$\downarrow$$

$$-Cg\left(r^\bullet,t^\bullet\right)\sum_{m=1}^{\infty^-}f_m\left(t^\bullet\right)\sin\left(m\left(\theta-z^\bullet/A\right)+\varphi_m\left(t^\bullet\right)\right)+Cg\left(r^\bullet,t^\bullet\right)\left\{\sum_{m=1}^{\infty^-}f_m\left(t^\bullet\right)\sin\left(m\left(\theta-z^\bullet/A\right)+\varphi_m\left(t^\bullet\right)\right)\right\}=0$$

$$\downarrow$$

$$0=0$$

$$\frac{1}{r^{\bullet}}\frac{\partial}{\partial r^{\bullet}}\left\{r^{\bullet}g\left(r^{\bullet},t^{\bullet}\right)\left\{\sum_{m=1}^{\infty^{-}}f_m\left(t^{\bullet}\right)\sin\left(m\left(\theta-z^{\bullet}/A\right)+\varphi_m\left(t^{\bullet}\right)\right)\right\}\right\}$$
$$+\frac{1}{r^{\bullet}}\frac{\partial}{\partial\theta}\left\{g\left(r^{\bullet},t^{\bullet}\right)\left\{\sum_{m=1}^{\infty^{-}}\left(\beta_m\left(r^{\bullet},t^{\bullet}\right)-f_m\left(t^{\bullet}\right)B\theta\right)\sin\left(m\left(\theta-z^{\bullet}/A\right)+\varphi_m\left(t^{\bullet}\right)\right)\right\}\right\}$$
$$+\frac{\partial}{\partial z^{\bullet}}\left\{\sum_{m=1}^{\infty^{-}}f_m\left(t^{\bullet}\right)\left(h\left(r^{\bullet},t^{\bullet}\right)-g\left(r^{\bullet},t^{\bullet}\right)C\theta\right)\sin\left(m\left(\theta-z^{\bullet}/A\right)+\varphi_m\left(t^{\bullet}\right)\right)\right\}=0 \tag{35}$$

Or, performing the required differentiation and simplifying, yields

$$\frac{1}{r^{\bullet}}\frac{\partial}{\partial r^{\bullet}}\left(r^{\bullet}g\left(r^{\bullet},t^{\bullet}\right)\right)\cdot\left\{\sum_{m=1}^{\infty^{-}}f_m\left(t^{\bullet}\right)\sin\left(m\left(\theta-z^{\bullet}/A\right)+\varphi_m\left(t^{\bullet}\right)\right)\right\}$$
$$+g\left(r^{\bullet},t^{\bullet}\right)\left\{\sum_{m=1}^{\infty^{-}}\frac{mz^{\bullet}}{A^2}\frac{\partial A}{\partial r^{\bullet}}\cdot f_m\left(t^{\bullet}\right)\cos\left(m\left(\theta-z^{\bullet}/A\right)+\varphi_m\left(t^{\bullet}\right)\right)\right\}$$
$$-B\frac{g\left(r^{\bullet},t^{\bullet}\right)}{r^{\bullet}}\left\{\sum_{m=1}^{\infty^{-}}f_m\left(t^{\bullet}\right)\sin\left(m\left(\theta-z^{\bullet}/A\right)+\varphi_m\left(t^{\bullet}\right)\right)\right\}$$
$$+\frac{g\left(r^{\bullet},t^{\bullet}\right)}{r^{\bullet}}\left\{\sum_{m=1}^{\infty^{-}}m\left(\beta_m\left(r^{\bullet},t^{\bullet}\right)-f_m\left(t^{\bullet}\right)B\theta\right)\cos\left(m\left(\theta-z^{\bullet}/A\right)+\varphi_m\left(t^{\bullet}\right)\right)\right\}$$
$$-\left\{\sum_{m=1}^{\infty^{-}}\frac{m}{A}f_m\left(t^{\bullet}\right)\left(h\left(r^{\bullet},t^{\bullet}\right)-g\left(r^{\bullet},t^{\bullet}\right)C\theta\right)\cos\left(m\left(\theta-z^{\bullet}/A\right)+\varphi_m\left(t^{\bullet}\right)\right)\right\}=0 \tag{36}$$

The above equation, after collecting sinusoidal terms that are in common, and by necessity setting each collected subset of terms to zero, decomposes into four simpler equations/relationships[‡‡‡]

$$\frac{\partial}{\partial r^{\bullet}}\left(g\left(r^{\bullet},t^{\bullet}\right)\right)+\frac{(1-B)}{r^{\bullet}}g\left(r^{\bullet},t^{\bullet}\right)=0$$

$$h\left(r^{\bullet},t^{\bullet}\right)\propto\frac{A}{r^{\bullet}}g\left(r^{\bullet},t^{\bullet}\right)$$

And

---

‡‡‡ As an aside, it should be noted that the vorticity divergence relationship is automatically satisfied as continuity is satisfied when length scale factors are used to linearly relate the vorticity and velocity components, i.e.

$$div\boldsymbol{\omega}\equiv\nabla\cdot\boldsymbol{\omega}=0$$
$$\downarrow$$
$$\frac{1}{r}\frac{\partial}{\partial r}\left(r\hat{\omega}_r\right)+\frac{1}{r}\frac{\partial\hat{\omega}_\theta}{\partial\theta}+\frac{\partial\hat{\omega}_z}{\partial z}=-\frac{1}{\ell}\left\{\frac{1}{r}\frac{\partial}{\partial r}\left(r\hat{v}_r\right)+\frac{1}{r}\frac{\partial\hat{v}_\theta}{\partial\theta}+\frac{\partial\hat{v}_z}{\partial z}\right\}=0$$

$$\sum_{m=1}^{\infty^-} a \cdot m \cdot \chi(m) \to 0$$

While

$$\sum_{m=1}^{\infty^-} a \cdot \chi(m) \to nonzero\ \ constant$$

(37a-d)

In the above, a is an arbitrary constant with respect to the mode number, m. Note that the first constraint, Eq. 37a, defines an absolute condition for preserving continuity. The second constraint, Eq. 37b, is not absolute; instead it establishes an implied proportional relationship of $h\left(r^\bullet, t^\bullet\right)$ in terms of $g\left(r^\bullet, t^\bullet\right)$. The reason why the second constraint establishes only an implied proportional rather than an equivalence relationship between $h\left(r^\bullet, t^\bullet\right)$ and $g\left(r^\bullet, t^\bullet\right)$ is because the third and fourth constraints, Eq. 37c-d, must be absolutely satisfied and, in fact, take precedence over any relationship that might be defined between $h\left(r^\bullet, t^\bullet\right)$ and $g\left(r^\bullet, t^\bullet\right)$. In this regards, $h\left(r^\bullet, t^\bullet\right)$ might be considered a semi-arbitrary function. It is this semi-arbitrariness that provides the analytic flexibility to introduce additional terms/functionality in order to satisfactorily deal with the otherwise singular behavior of $h\left(r^\bullet, t^\bullet\right)$ at $r^\bullet = 0$. The third and fourth derived constraints, Eq. 37c-d, are quite unique. For the higher modes ($m \geq 1$), continuity is not satisfied on a mode-by-mode basis but instead must be considered as an aggregate/cumulative result. A possible alternate constraint, $B = Cr^\bullet / A$, cannot be expected to be universally satisfied by any given vortex basic flow and so is discarded as a means of enforcing continuity. The third and fourth higher-mode constraints have profound implications as to the functional dependence of $f_m\left(t^\bullet\right)$, as it has the functional dependence of $f_m\left(t^\bullet\right) \propto \chi(m)$, with respect to the mode number. Essentially, the third and four constraints, Eq. 37c-d, dictate convergence properties of any given series, or rather finite sum, comprised of $f_m\left(t^\bullet\right)$. Note that as $\beta_m\left(r^\bullet, t^\bullet\right) \propto f_m\left(t^\bullet\right) \propto \chi(m)$, these higher-mode continuity constraints equally apply to $\beta_m\left(r^\bullet, t^\bullet\right)$, as well.

Recognizing that the turbulent fluctuation solution series expressions can be truncated at an arbitrary integer, M, chosen to represent the asymptotic approach to the limit $m \to \infty^-$, then M can be prescribed to be an even integer, $m \to 2 \cdot \lfloor M/2 \rfloor$ without any significant loss of generality. Note that $\lfloor x \rfloor$, or $floor(x)$, is the well-known "floor" function, which takes a real number and returns the closest lower-in-value integer to the original real number; i.e., if x is a real number, and j is an integer, such that $j \leq x < j+1$ then $\lfloor x \rfloor = j$. Therefore, for the turbulent fluctuation velocity solutions, each mode will be a member of a subset of modes such that $\cos\left(M_1 x + \lambda_{M_1}\right) = \cos\left(M_2 x + \lambda_{M_2}\right) = \ldots = \cos\left(M_k x + \lambda_{M_k}\right)$ where $M_k = M_1 + \left\lfloor \left(2\pi(k-1) + \lambda_{M_1} - \lambda_{M_k}\right) / x \right\rfloor$. Note the recursive nature of this modal relationship. If $\left\lfloor \left(2\pi(k-1) + \lambda_{M_1} - \lambda_{M_k}\right) / x \right\rfloor < \lfloor 2\pi(k-1)/x \rfloor$, or rather $\lambda_k << \pi/2$ for all k, then the recursive modal relationship is explicit, rather than implicit, in nature. This taken altogether allows for continuity to be approximately satisfied in an aggregate/collective manner for the higher modes. There are perhaps an infinite number of possible functional series with the required convergent properties. Arguably, the simplest choice for such a series, however, is the one advanced in this paper for application to the present problem. Proceeding in this manner, the third and fourth higher-mode continuity constraints can be captured by the following alternating sum expression

$$\chi(m) = \frac{(-1)^{m+1}}{m}$$

Such that, as assumed earlier $f_m\left(t^\bullet\right) = \chi(m) f\left(m, t^\bullet\right)$, the following holds

$$f_m\left(t^\bullet\right) = \frac{(-1)^{m+1}}{m} f\left(m, t^\bullet\right)$$

(38a-b)

This expression can be seen to readily to satisfy the third and fourth constraint for continuity, for the higher modes, as long as, in addition to the other limitations noted above, $f\left(m, t^\bullet\right)$ is not separable with respect to m and $t^\bullet$. I.e., $f\left(m, t^\bullet\right)$ is not separable in the sense that multiplier terms of the form m^j, where j is any arbitrary integer such that $j \neq 0$, cannot generally be extracted it. If $f\left(m, t^\bullet\right)$ were separable in this unique sense, such that m^j multiplier terms could be extracted, then the desired convergence properties for the overall functional series would be lost and higher-mode continuity could not be satisfied.

Given this higher-mode functionality of $f\left(m, t^\bullet\right)$ and $\beta_m\left(r^\bullet, t^\bullet\right)$, the result as to the turbulent fluctuation velocities is as follows

$$\hat{v}_r^\bullet = g\left(r^\bullet, t^\bullet\right)\left\{\sum_{m=1}^{M} \frac{(-1)^{m+1}}{m} f\left(m, t^\bullet\right) \sin\left(m\left(\theta - z^\bullet / A\right) + \varphi_m\left(t^\bullet\right)\right)\right\}$$

$$\hat{v}_\theta^\bullet = g\left(r^\bullet, t^\bullet\right)\left\{\sum_{m=1}^{M} \frac{(-1)^{m+1}}{m} \left(\varepsilon\left(m, r^\bullet, t^\bullet\right) + f\left(m, t^\bullet\right)(1 - B\theta)\right) \sin\left(m\left(\theta - z^\bullet / A\right) + \varphi_m\left(t^\bullet\right)\right)\right\}$$

$$\hat{v}_z^\bullet = \left(h\left(r^\bullet, t^\bullet\right) - g\left(r^\bullet, t^\bullet\right) C\theta\right)\left\{\sum_{m=1}^{M} \frac{(-1)^{m+1}}{m} f\left(m, t^\bullet\right) \sin\left(m\left(\theta - z^\bullet / A\right) + \varphi_m\left(t^\bullet\right)\right)\right\}$$

Where

$$M = 2 \cdot \lfloor M/2 \rfloor$$

(39a-d)

Having gained improved insight into the higher-mode functional dependence (with respect to θ and $z^\bullet$) of $\hat{v}_r^\bullet$, $\hat{v}_\theta^\bullet$, and $\hat{v}_z^\bullet$, the functionality with respect to the radial coordinate, $r^\bullet$, will now be examined. Solving Eq. 37a gives the expression

$$g\left(r^\bullet, t^\bullet\right) \approx \frac{\eta}{r^\bullet} \cdot \exp\left(\int \left(B / r^\bullet\right) dr^\bullet\right) \varsigma(A)$$

Where

$$\varsigma(A) \equiv \begin{cases} u\left(|A| - \alpha\right) \\ or \\ \varsigma(m, A) = \dfrac{1}{2}\left\{1 + erf\left(\kappa_0 m\left(|A| - \alpha\right)\right)\right\} \end{cases}$$

(40a-b)

Where η is an arbitrary constant with respect to $r^\bullet$. The first formulation for $\varsigma(A)$ is a discontinuous cut-off of the vortex turbulent fluctuation; this is all that the governing equations, Eq. 15a-c, can explicitly reveal about the dependence of the radial "boundary" of the turbulence distribution with respect to the parameter A. However, it more physically realistic to anticipate that some sort of smoothing of this turbulence cut-off boundary occurs, in this case an arbitrary smoothing function is defined with the second functional formulation for $\varsigma(A)$, with κ_0 an arbitrary constant defining the effective slope of the smoothing function. When the mean flow parameter A drops below a certain value the turbulence is assumed to drop to zero and/or some background level. The governing cut-off constant, α, is set to some small value. For the work performed in this paper $\alpha < 10^{-4}$. Application of this cut-off function is analytically justified in that the governing turbulent fluctuation linear partial differential equations, Eq. 15a-c, fundamentally change in nature as $A \to 0$. Application of the cut-off parameter α, in this context, is analogous to defining displacement and/or momentum thicknesses in classic integral boundary-layer theory. Note that a modal dependency, the coefficient m in the error function term, has been introduced in the second formulation of the cut-off function. This modal dependency is essential for preserving continuity, while at the same time smoothing out any jumps in turbulence in the outer "boundary" of the vortex.

Given Eq. 23b for B, the following holds

$$\begin{aligned} g\left(r^\bullet,t^\bullet\right) &\approx \frac{\eta}{r^\bullet}\cdot\exp\left(\int\left(B/r^\bullet\right)dr^\bullet\right)\varsigma(A) \approx \frac{\eta}{r^\bullet}\cdot\exp\left(\int\frac{1}{r^\bullet}\left(\frac{-r^\bullet}{v_\theta^\bullet}\frac{\partial v_\theta^\bullet}{\partial r^\bullet}\right)dr^\bullet\right)\varsigma(A) \\ &\approx \frac{\eta}{r^\bullet}\cdot\exp\left(-\int\frac{1}{v_\theta^\bullet}\,dv_\theta^\bullet\right)\varsigma(A) \approx \frac{\eta}{r^\bullet}\cdot\exp\left(-\ln\left(v_\theta^\bullet\right)\right)\varsigma(A) \\ &\approx \frac{\eta\varsigma(A)}{r^\bullet v_\theta^\bullet} \end{aligned} \tag{41}$$

The above expression for $g\left(r^\bullet,t^\bullet\right)$ satisfies Eq. 37a, and therefore its contribution to preserving continuity, but it exhibits a non-physical singularity at $r^\bullet = 0$. This problem can be eliminated by re-introducing a modal dependence into $g\left(r^\bullet,t^\bullet\right)$, i.e. $g\left(r^\bullet,t^\bullet\right) \to g\left(m,r^\bullet,t^\bullet\right)$, and then applying the higher-mode continuity constraints to $g\left(m,r^\bullet,t^\bullet\right)$. Note that re-introduction of a modal dependence to $g\left(r^\bullet,t^\bullet\right)$ does not conflict with the earlier analysis results in the paper. Therefore, given the Eq. 41 result, the derived functional relationship is recast with added exponential terms to de-singularize it.

$$g\left(m,r^\bullet,t^\bullet\right) = \frac{\eta}{r^\bullet v_\theta^\bullet}\lambda\left(m,r^\bullet\right)\varsigma(A)$$

Where it is conjectured that the functionality of the $\lambda(m,r)$ multiplier function is given by

$$\lambda(m,r) \equiv \left\{\left(1-u\left(1-r^\bullet\right)\right)+\left(r^\bullet\right)^{2m}\cdot\exp\left(1-\left(r^\bullet\right)^2\right)\cdot u\left(1-r^\bullet\right)\right\} \tag{42a-b}$$

This recast formulation of the radial distribution eliminates the singularity at $r^\bullet = 0$ without violating continuity. As a minimum, the functionality of $\lambda(m,r)$ must accommodate the following requirements:

$\partial\left(\lambda\left(m,r^{\bullet}\right)\right)\Big/\partial r^{\bullet} \propto m\lambda^{*}\left(r^{\bullet}\right)$, $\partial\left(\lambda\left(m,r^{\bullet}\right)\right)\Big/\partial r^{\bullet} \le 0$ throughout the range $0 \le r^{\bullet} < 1$, $\lambda(1,r) \propto \left(r^{\bullet}\right)^{2}$ as $r^{\bullet} \to 0$, and $\lambda(m,r) = 1$ as $r^{\bullet} = 1$. Additionally note the required functionality of the cut-off function, i.e. $\partial\left(\varsigma(m,A)\right)\Big/\partial r^{\bullet} \propto m\varsigma^{*}(A)$.[§§§]

The semi-arbitrary functional relationship, Eq. 37b, for the $h\left(r^{\bullet},t^{\bullet}\right)$ needs to be augmented with a more precise means of derivation, this will be accomplished by considering the vorticity component definitions directly. The derivation of the following equation is detailed in Appendix C. In summary, though, this more precise relationship is

$$\frac{\partial}{\partial r^{\bullet}} h\left(m,r^{\bullet},t^{\bullet}\right) + \left\{1 + d_m \cdot (1+A)\right\} g\left(m,r^{\bullet},t^{\bullet}\right) \approx 0 \tag{43}$$

Note that a modal dependence is intrinsic to this function, i.e. $h\left(r^{\bullet},t^{\bullet}\right) \to h\left(m,r^{\bullet},t^{\bullet}\right)$. Further, the ratio of the functions $\varepsilon\left(m,r^{\bullet},t^{\bullet}\right)$ and $f\left(m,t^{\bullet}\right)$ have been approximated by means of the introduction of the modal constants d_m as well as retention of the prescribed radial function of $\varepsilon\left(m,r^{\bullet},t^{\bullet}\right)$, i.e. $\varepsilon\left(m,r^{\bullet},t^{\bullet}\right) \propto 1 + A$.

In general, Eq. 43 does not appear analytically tractable. It could, of course, be solved for numerically, but an alternate, approximate analytical approach is instead proposed. From previous work, Eq. 37b, a semi-arbitrary partial solution to $h\left(r^{\bullet},t^{\bullet}\right)$, i.e. $h\left(r^{\bullet},t^{\bullet}\right) \propto Ag\left(m,r^{\bullet},t^{\bullet}\right)\Big/r^{\bullet}$ has been defined. Given this earlier result, it is assumed that the complete solution for $h\left(r^{\bullet},t^{\bullet}\right)$ is of the form

---

[§§§] The higher-mode continuity constraints, Eq. 37c-d, are key to the desingularization of Eq. 41. This will be validated by direction of Eq. 42a into Eq. 37a. Essentially, continuity in the inner core of the vortex, for $r^{\bullet} < 1$, is fully contingent upon exercising the higher-mode continuity constraints previously identified. For $r^{\bullet} \ge 1$ the higher-mode continuity constraints do not need to be invoked to satisfy continuity

$$\frac{\partial}{\partial r^{\bullet}}\left(g\left(m,r^{\bullet},t^{\bullet}\right)\right) + \frac{(1-B)}{r^{\bullet}} g\left(m,r^{\bullet},t^{\bullet}\right) = 0$$

$$\downarrow$$

$$\frac{\partial}{\partial r^{\bullet}}\left(\frac{\eta}{r^{\bullet}v_{\theta}^{\bullet}}\lambda\left(m,r^{\bullet}\right)\varsigma(A)\right) + \frac{(1-B)}{r^{\bullet}}\frac{\eta}{r^{\bullet}v_{\theta}^{\bullet}}\lambda\left(m,r^{\bullet}\right)\varsigma(A) = 0$$

$$\downarrow$$

$$\left\{-\frac{\eta}{\left(r^{\bullet}\right)^{2}v_{\theta}^{\bullet}} - \frac{\eta}{r^{\bullet}\left(v_{\theta}^{\bullet}\right)^{2}}\frac{\partial v_{\theta}^{\bullet}}{\partial r^{\bullet}} + \eta\frac{(1-B)}{r^{\bullet}}\left(\frac{1}{r^{\bullet}v_{\theta}^{\bullet}}\right)\right\}\lambda\left(m,r^{\bullet}\right)\varsigma(A) + \frac{\eta}{r^{\bullet}v_{\theta}^{\bullet}}\varsigma(A)\frac{\partial}{\partial r^{\bullet}}\left(\lambda\left(m,r^{\bullet}\right)\right) + \frac{\eta}{r^{\bullet}v_{\theta}^{\bullet}}\lambda\left(m,r^{\bullet}\right)\frac{\partial}{\partial r^{\bullet}}\left(\varsigma(A)\right) = 0$$

$$\downarrow$$

$$\left\{-\frac{\eta}{\left(r^{\bullet}\right)^{2}v_{\theta}^{\bullet}} + \frac{\eta B}{\left(r^{\bullet}\right)^{2}v_{\theta}^{\bullet}} + \frac{\eta}{\left(r^{\bullet}\right)^{2}v_{\theta}^{\bullet}} - \frac{\eta B}{\left(r^{\bullet}\right)^{2}v_{\theta}^{\bullet}}\right\}\lambda\left(m,r^{\bullet}\right)\varsigma(A) + m\cdot\frac{\eta}{r^{\bullet}v_{\theta}^{\bullet}}\varsigma(A)\lambda^{*}\left(r^{\bullet}\right) + m\cdot\frac{\eta}{r^{\bullet}v_{\theta}^{\bullet}}\lambda\left(m,r^{\bullet}\right)\varsigma^{*}(A) = 0$$

$$\downarrow$$

$$m\cdot\left\{\frac{\eta}{r^{\bullet}v_{\theta}^{\bullet}}\varsigma(A)\lambda^{*}\left(r^{\bullet}\right) + \frac{\eta}{r^{\bullet}v_{\theta}^{\bullet}}\lambda\left(m,r^{\bullet}\right)\varsigma^{*}(A)\right\} = 0$$

Because the residual terms of the Eq. 37a have coefficients of m modal number, therefore, application of the higher-mode continuity constraints, Eq. 37c-d, will cause these terms to vanish as the modal contributions to the continuity equation are considered in an aggregate (even-order finite-sum) manner.

$$h\left(m,r^{\bullet},t^{\bullet}\right)=\frac{A}{r^{\bullet}+\xi\left(m,r^{\bullet}\right)}g\left(m,r^{\bullet},t^{\bullet}\right)+c \tag{44}$$

Where c is an arbitrary constant, and, further, $\xi\left(m,r^{\bullet}\right)$ is an unknown function that will be solved for in the following analysis.

Substituting Eq. 37b into Eq. 43 yields the following

$$\frac{\partial\xi}{\partial r^{\bullet}}-\left(r^{\bullet}+\xi\right)\cdot\frac{1}{A}\frac{\partial A}{\partial r^{\bullet}}-\left(r^{\bullet}+\xi\right)\cdot\frac{1}{g}\frac{\partial g}{\partial r^{\bullet}}-\frac{1}{A}\left(r^{\bullet}+\xi\right)^{2}\left\{1+d_m\cdot\left(1+A\right)\right\}+1=0 \tag{45}$$

Where, for brevity, the following abbreviated nomenclature is employed: $\xi\equiv\xi\left(m,r^{\bullet}\right)$ and $g\equiv g\left(m,r^{\bullet},t^{\bullet}\right)$. The unknown function $\xi\left(m,r^{\bullet}\right)$ is of negligible magnitude except as $r^{\bullet}\to 0$; therefore, Eq. 45 will only be evaluated, in asymptotic sense, at $r^{\bullet}\to 0$. At this asymptotic condition, the following limit values are approached for the various quantities contained in Eq. 45: (1) $\xi\to constant$, (2) $A\to -1$, (3) $\partial A/\partial r^{\bullet}\to 0$, (4) $g\to constant$, and (5) $\partial g/\partial r^{\bullet}\to 0$. Therefore, given the asymptotic behavior of these key parameters, Eq. 45 reduces to the following simple ordinary differential equation

$$\frac{\partial\xi}{\partial r^{\bullet}}+\xi^{2}+1\approx 0 \tag{46}$$

The above ordinary differential equation is a particular case of the special Riccati equation. This equation has a simple solution applicable to the problem being studied, which is $\xi=\xi\left(m,r^{\bullet}\right)=\xi\left(r^{\bullet}\right)=\cot\left(r^{\bullet}\right)$. This solution must be limited in application to the range $0<r^{\bullet}<\sim 4\pi/5$ in order to avoid a non-physical sign reversal in $h\left(m,r^{\bullet},t^{\bullet}\right)$. Further, the constant c has been set to zero. Therefore, the final form of the $h\left(m,r^{\bullet},t^{\bullet}\right)$ expression is

$$h\left(m,r^{\bullet},t^{\bullet}\right)\approx\frac{A}{r^{\bullet}+\cot\left(r^{\bullet}\right)}g\left(m,r^{\bullet},t^{\bullet}\right) \tag{47}$$

Some of the time functionality of the turbulent flow is captured in the derivation of the expression for $g\left(r^{\bullet},t^{\bullet}\right)$. However, this is, so far, only a partial solution. The remaining functionality with respect to time for the turbulent fluctuation velocities $\hat{v}_r^{\bullet}$, $\hat{v}_{\theta}^{\bullet}$, and $\hat{v}_z^{\bullet}$ needs to be defined in terms of the additional time-dependent functions $f\left(m,t^{\bullet}\right)$ and $\varphi_m\left(t^{\bullet}\right)$. This will partly be accomplished by first noting that, though the large-Reynolds-number approximation was initially invoked to derive the turbulent fluctuation velocity solutions, ideally the heat conduction equation for all three velocity components should be (at least approximately) satisfied, so as to approximately satisfy the complete Helmholtz vorticity transport equations. Relying on the trigonometric identity, $\sin\left(x\pm y\right)=\sin x\cos y\pm\cos x\sin y$, as partially or quasi separable solutions for the turbulent fluctuation velocities have been derived, therefore the turbulent fluctuation velocity solutions can be recast as

$$\hat{v}_r^{\bullet} = \sum_m f_m\left(t^{\bullet}\right)\cos\left(\varphi_m\left(t^{\bullet}\right)\right)\tilde{\Psi}_1\left(m,\theta,r^{\bullet},z^{\bullet},t^{\bullet}\right) + f_m\left(t^{\bullet}\right)\sin\left(\varphi_m\left(t^{\bullet}\right)\right)\tilde{\Psi}_2\left(m,\theta,r^{\bullet},z^{\bullet},t^{\bullet}\right)$$
$$\approx \sum_m f_m\left(t^{\bullet}\right)\cos\left(\varphi_m\left(t^{\bullet}\right)\right)\Psi_1\left(m,\theta,r^{\bullet},z^{\bullet}\right) + f_m\left(t^{\bullet}\right)\sin\left(\varphi_m\left(t^{\bullet}\right)\right)\Psi_2\left(m,\theta,r^{\bullet},z^{\bullet}\right)$$

$$\hat{v}_\theta^{\bullet} = \sum_m f_m\left(t^{\bullet}\right)\cos\left(\varphi_m\left(t^{\bullet}\right)\right)\tilde{\Omega}_1\left(m,\theta,r^{\bullet},z^{\bullet},t^{\bullet}\right) + f_m\left(t^{\bullet}\right)\sin\left(\varphi_m\left(t^{\bullet}\right)\right)\tilde{\Omega}_2\left(m,\theta,r^{\bullet},z^{\bullet},t^{\bullet}\right)$$
$$\approx \sum_m f_m\left(t^{\bullet}\right)\cos\left(\varphi_m\left(t^{\bullet}\right)\right)\Omega_1\left(m,\theta,r^{\bullet},z^{\bullet}\right) + f_m\left(t^{\bullet}\right)\sin\left(\varphi_m\left(t^{\bullet}\right)\right)\Omega_2\left(m,\theta,r^{\bullet},z^{\bullet}\right)$$

$$\hat{v}_z^{\bullet} = \sum_m f_m\left(t^{\bullet}\right)\cos\left(\varphi_m\left(t^{\bullet}\right)\right)\tilde{\mathrm{X}}_1\left(m,\theta,r^{\bullet},z^{\bullet},t^{\bullet}\right) + f_m\left(t^{\bullet}\right)\sin\left(\varphi_m\left(t^{\bullet}\right)\right)\tilde{\mathrm{X}}_2\left(m,\theta,r^{\bullet},z^{\bullet},t^{\bullet}\right)$$
$$\approx \sum_m f_m\left(t^{\bullet}\right)\cos\left(\varphi_m\left(t^{\bullet}\right)\right)\mathrm{X}_1\left(m,\theta,r^{\bullet},z^{\bullet}\right) + f_m\left(t^{\bullet}\right)\sin\left(\varphi_m\left(t^{\bullet}\right)\right)\mathrm{X}_2\left(m,\theta,r^{\bullet},z^{\bullet}\right)$$

(48a-c)

Derivation of the $f_m(t^{\bullet})$ functions is critically important. If left unchecked, without $f_m(t^{\bullet})$, the turbulent kinetic energy would eventually grow infinitely large. This is, of course, not physically valid. A "relatively quasi-steady" approximation is implied in Eq. 48a-c, i.e. $\tilde{\mathbf{U}}_1 \to \dot{\mathbf{U}}_1$, $\tilde{\mathbf{X}}_1 \to \mathbf{X}_1$, etc. "Relatively quasi-steady," in this particular context, implies that $\partial\left(f_m(t^{\bullet})\right)/\partial t^{\bullet} >> \partial\tilde{\mathbf{U}}_1/\partial t^{\bullet}$, $\partial\left(f_m(t^{\bullet})\right)/\partial t^{\bullet} >> \partial\tilde{\mathbf{X}}_1/\partial t^{\bullet}$, etc. This is reasonable assumption for two reasons. First, $\partial\left(f_m(t^{\bullet})\right)/\partial t^{\bullet}$ must be large in order to check growth in turbulent kinetic energy and keep it from becoming infinite in magnitude. Second, $f_m(t^{\bullet})$ is the means by which high-frequency oscillatory content is introduced for the turbulent fluctuations; this oscillatory contribution, by definition, implies large values, in terms of absolute magnitude, of $\partial\left(f_m(t^{\bullet})\right)/\partial t^{\bullet}$. Given this, if the following approximations are reasonably accurate

$$\nabla^2\Psi_1 - C_\Psi\Psi_1 \approx 0 \qquad \text{And} \qquad \nabla^2\Psi_2 - C_\Psi\Psi_2 \approx 0$$

$$\nabla^2\Omega_1 - C_\Omega\Omega_1 \approx 0 \qquad \text{And} \qquad \nabla^2\Omega_2 - C_\Omega\Omega_2 \approx 0$$

$$\nabla^2\mathrm{X}_1 - C_\mathrm{X}\mathrm{X}_1 \approx 0 \qquad \text{And} \qquad \nabla^2\mathrm{X}_2 - C_\mathrm{X}\mathrm{X}_2 \approx 0$$

(49a-f)

Where C_Ψ, C_Ω, C_X, etc are arbitrary constants in the above; these constants are an assumed consequence of the differentiation operations in the Laplacian. Then, as a consequence of the heat conduction equation requirement, and the length scale factor velocity and vorticity linear relationships, the following should hold

$$\frac{\partial}{\partial t^{\bullet}}\left(f_m\left(t^{\bullet}\right)\cos\left(\varphi_m\left(t^{\bullet}\right)\right)\right) - C\cdot f_m\left(t^{\bullet}\right)\cos\left(\varphi_m\left(t^{\bullet}\right)\right) \approx 0$$

$$\frac{\partial}{\partial t^{\bullet}}\left(f_m\left(t^{\bullet}\right)\sin\left(\varphi_m\left(t^{\bullet}\right)\right)\right) - C\cdot f_m\left(t^{\bullet}\right)\sin\left(\varphi_m\left(t^{\bullet}\right)\right) \approx 0$$

(50a-b)

The functionality of $\tilde{\Psi}_1$, $\tilde{\Psi}_2$, $\tilde{\Omega}_1$, $\tilde{\Omega}_2$, $\tilde{\mathrm{X}}_1$, and $\tilde{\mathrm{X}}_2$ have already been pre-established with the analysis performed earlier. C is an arbitrary constant required to be consistent with the assumed approximate requirements, Eq. 48a-c, necessary to satisfy the spatial aspects of the heat conduction equation. However,

to some degree, the accuracy of the resulting spatial approximation has only a secondary influence on the validity of Eq. 50a-b and, in turn, the temporal functionality of the turbulent fluctuation solutions.

It will be assumed that $\varphi_m\left(t^\bullet\right)$ is a stochastic function estimated at discrete instantiations and, therefore, does not have any time dependency in a conventional sense. Therefore, the time derivative as applied to terms containing $\varphi_m\left(t^\bullet\right)$ in Eq. 50a-b can be ignored. Therefore, Eq. 50a-b reduces to

$$\begin{gathered}\frac{\partial}{\partial t^\bullet}\left(f_m\left(t^\bullet\right)\right)-C_m f_m\left(t^\bullet\right)\approx 0 \\ \downarrow \\ \frac{\partial}{\partial t^\bullet}\left(f\left(m,t^\bullet\right)\right)-C_m f\left(m,t^\bullet\right)\approx 0\end{gathered} \tag{51}$$

Given the above simple first-order ordinary differential equation, and noting that the elemental solution is $f\left(m,t^\bullet\right)\propto\alpha_m e^{C_m t^\bullet}$, C_m can represent a set of constants comprised of complex numbers. Therefore, the complete time functionality can be described in following general series form

$$f\left(m,t^\bullet\right)\approx\sum_{n=1}^{N}\alpha_{mn}\left(e^{-a_{mn}t^\bullet}-e^{-b_{mn}t^\bullet}\right)\cos\left(c_{mn}t^\bullet\right)w_P \tag{52}$$

Note that, in the above, that for each m[th] mode there are $1\le n\le N$ series terms that define $f\left(m,t^\bullet\right)$. Further, the series is comprised of exponential and sinusoidal terms (recognizing that the complete solution can be comprised of the product of exponentials having complex number arguments). The coefficients, c_{mn}, in the sinusoidal terms represent the "modal" natural frequencies for the turbulent fluctuations. Lower modal frequencies correspond to coherent structures in the flow. Higher modal frequencies correspond to isotropic homogeneous turbulence. A natural fundamental frequency, Ω, of the flow is given by $\Omega=v_\theta/2\pi r\big|_{\substack{r=r_{c0}\\ t\to 0}}$ or $\Omega\approx\gamma/\left(2\pi r_{c0}\right)^2$ for an initially uniform vorticity distribution. This fundamental frequency is sometimes referred to as the "turn over rate," e.g. Ref. 3. It follows that a nondimensional version of Ω is given by $\Omega^\bullet=\mathrm{Re}/\left(2\pi\right)^2$. The coefficients c_{mn} can be related to this proposed fundamental frequency by the assumed expression $c_{mn}\propto n\Omega^\bullet$. The anticipated initial and final conditions for the turbulent fluctuations are: (1) for $t^\bullet=0$, then $f\left(m,t^\bullet\right)=0$, i.e. the flow is initially laminar; (2) for $t^\bullet\to\infty$, then $f\left(m,t^\bullet\right)\approx constant\cdot\cos\left(c_{mn}t^\bullet\right)$ where some (higher mode) fluctuations have not dampened out, or, alternatively, $f\left(m,t^\bullet\right)=0$ where the (mid-range mode) fluctuations have dampened out. This further dictates that $a_{mn}<b_{mn}$ -- where, in most cases, the difference in value between the two coefficients is quite small. i.e. $a_{mn}\to b_{mn}^-$. Specifically, it is anticipated that $a_{mn}\to b_{mn}-\varepsilon/\left(1+n\right)$ where ε is some small arbitrary constant offsetting the two sets of coefficient values. This sensitivity of the relative ratio of the coefficients b_{mn} and a_{mn} -- as to turbulent fluctuations dampening out or continuing to sustain oscillations -- implies a critical sensitivity to initial condition that is a key feature of turbulent flows in general. To yield a convergent series, to avoid infinite turbulent kinetic energy, it is also required that $\alpha_{mn}\propto 1/\left(1+n\right)^x$ where, as a minimum, $x\le 1$. The assignment of specific values for x has significant implications for the resulting estimates of the turbulence energy spectrum. Additionally, note the introduction of a stochastic function, w_P. This stochastic function returns a random

value for each instantiation, or a point-wise (spatiotemporally) estimate, of the turbulent fluctuation velocity; further, a normal distribution is assumed for w_P, where the distribution is centered about $w_P = 1$.

The analysis for deriving the functionality of the turbulent fluctuation velocities is complete except for defining the unknown constants and coefficients incorporated in the analysis. A major future challenge for the analysis methodology, which is outside the scope of this paper, is the rigorous definition of the coefficients included in the function $f\left(m, t^{\bullet}\right)$ and other constants/parameters identified along the way. Resolution of this problem will be dependent, in part, in defining physically relevant initial and asymptotic value conditions for the mean flow behavior of the turbulent vortex model. But, there is also the issue of how to define the higher-mode coefficients. It is likely that the approach for defining these unknown constant coefficients for the derived analytical expressions for the turbulent fluctuation velocities, $\hat{v}_r^{\bullet}$, $\hat{v}_\theta^{\bullet}$, and $\hat{v}_z^{\bullet}$ will still need to be semi-empirical in nature as it is in other turbulent flow models, and turbulence closure schemes, in general.

Next, the derivation of the turbulent mean flow contribution, Δv_{θ_T}, will now be performed. It is at this point in the paper that deterministic solutions have to give way to analysis based on stochastic processes. The following holds

$$\Delta v_{\theta_T} = \frac{1}{T}\int_{t}^{t+T} \hat{v}_\theta \, d\tau \tag{53}$$

Where T is some small, but statistically relevant, incremental period of time to perform the time integration of the turbulent fluctuation solution to yield the mean flow. The above integral is evaluated in some arbitrary $\theta - z$ plane. Note, additionally, that as a consequence of the length scale factor

$$\Delta\omega_{\theta_T} = -\Delta v_{\theta_T} / \ell \neq 0 \tag{54}$$

In order to not invalidate the turbulent fluctuation governing equations, i.e. the set of three linear partial differential equation, Eq. 15a-c this contribution has to be assumed to be small, i.e. $\omega_\theta^{\bullet} = \Delta\omega_{\theta_T} << \left|\overline{\hat{\omega}_\theta^{\bullet}}\right|$, as noted earlier in the paper. Further, by definition, for the particular class of turbulent line vortex being studied that

$$\Delta\omega_{z_T} = \frac{1}{T}\int_{t}^{t+T} \hat{\omega}_z \, d\tau = -\frac{1}{\ell T}\int_{t}^{t+T} \hat{v}_z \, d\tau = -\Delta v_{z_T} / \ell = -v_z / \ell = 0 \tag{55}$$

The above is a direct consequence of the length scale factor methodology and the attendant assumptions implicit in the primary governing equations, Eq. 15a-c, used in this paper to derive the turbulent fluctuation solutions. Simply put, the particular turbulent vortex model derived in this paper has a normalized axial vorticity distribution that is invariant with respect to the turbulence state of the vortex, i.e. the axial vorticity distribution is laminar-like and, further, always equivalent to the laminar distribution derived in Appendix B. In turn, that also dictates that the vortex circulation distribution is also laminar-like. However, because of accelerated vortex "aging," as a result of the turbulent flow state, the axial vorticity and vortex circulation distributions have "diffused" significant more than would happen if the flow were wholly laminar. This will be discussed in more detail later.

Returning now to the tangential velocity turbulent mean flow derivation, the only way a net change in the tangential velocity profile can be effected is for there to be an effective skewed offset in the tangential velocity fluctuations, i.e. the turbulent fluctuations being on whole more positive than negative in sign.

Correspondingly, the reason why $v_r = v_z = 0$, or as a minimum $v_r^\bullet << \left|\overline{\hat{v}_r^\bullet}\right|$, $v_z^\bullet << \left|\overline{\hat{v}_z^\bullet}\right|$, $\omega_r^\bullet << \left|\overline{\hat{\omega}_r^\bullet}\right|$, and $\omega_\theta^\bullet << \left|\overline{\hat{\omega}_\theta^\bullet}\right|$. is because these turbulent velocity components, $\hat{v}_r$ and $\hat{v}_z$, are not skewed positive in a similar manner as was done for the $\hat{v}_\theta$ solution by means of the $\varepsilon\left(m,t^\bullet\right)$ function.

An analysis by means of stochastic calculus formalism will not be performed in this paper to define the mean turbulent flow properties. Instead an informal heuristic analysis will be performed. Assume for the moment that certain parameters/functions in the to-this-point deterministic framework can have an element of stochastic functionality incorporated into them. Specifically, it is assumed that the phase angle function $\varphi_m\left(t^\bullet\right)$ is either a continuous Brownian process or a discrete random-walk. There are other parameters/functions in the $\hat{v}_\theta$ solution that could have stochastic attributes to them, specifically $f\left(m,t^\bullet\right)$, in the form of the normal distribution random function w_p, but a phase angle Brownian "shifting," is asserted as the primary mechanism for yielding mean turbulent flow properties. Assume further that the integration time-period, T, is of sufficient duration such that Brownian shifting of the phase angle will result in a uniform probability distribution for the phase angle, across the feasible range of $0 \le \varphi_m\left(t^\bullet\right) < \pi$, when taking into account symmetry considerations. Note that $\varphi_m\left(t^\bullet\right)$ is estimated on an ensemble basis, i.e. it is estimated only once for each unique value of time and not for each spatiotemporal point. Further, as the mean turbulent flow should only be a function of radial coordinate, the radial distribution can be evaluated at arbitrary θ and $z^\bullet$ coordinates; for simplicity, those coordinates are chosen to be $\theta = 0$ and $z^\bullet = 0$. Accordingly, the following must hold true

$$\begin{aligned}\Delta v_{\theta_T}^\bullet &= \frac{1}{T^\bullet}\int_{t^\bullet}^{t^\bullet+T^\bullet}\left\{\sum_{m=1}^{M}\frac{(-1)^{m+1}}{m}g\left(m,r^\bullet,\tau\right)\left(\varepsilon(m,\tau)+f\left(m,\tau\right)(1-B\theta)\right)\sin\left(m\left(\theta-z^\bullet/A\right)+\varphi_m(\tau)\right)\right\}d\tau \\ &= \frac{1}{T^\bullet}\int_{t^\bullet}^{t^\bullet+T^\bullet}\left\{\sum_{m=1}^{M}\frac{(-1)^{m+1}}{m}g\left(m,r^\bullet,\tau\right)\left(\varepsilon(m,\tau)+f\left(m,\tau\right)\right)\sin\left(\varphi_m(\tau)\right)\right\}d\tau\end{aligned} \tag{56}$$

Assuming that each of the oscillatory and or stochastic functions have their own independent time-scale with respect to each other, therefore, each function can have a mean value associated with it that is independent with respect to the other oscillatory/stochastic functions. Given, that a mean value can be established for each oscillatory and/or stochastic function, the mean value theorem of integral calculus can be applied. As, $\varphi_m(\tau)$ is stochastically uniformly distributed over the range $0 \le \varphi_m\left(t^\bullet\right) < \pi$, a mean value substitution for the $\overline{\sin\left(\varphi_m(\tau)\right)} = (1/\pi)\int_0^\pi \sin x dx = 2/\pi$ term in the time-integral. Further, the mean flow contribution from the $f_m\left(t^\bullet\right)$ function can be directly evaluated if the coefficients in the function were fully enumerated, but a simpler approach and one more consistent with correlation with experimental turbulent vortex measurements is to subsume the functionality of the $f_m\left(t^\bullet\right)$ function – and its decomposed contributory elemental functions $\varepsilon\left(m,r^\bullet,\tau\right)$ and $f\left(m,\tau\right)$ -- into a RMS-like parameter, i.e. η_ε, or, more specifically, the nondimensional turbulence $\overline{f_m\left(t^\bullet\right)} \propto \eta_\varepsilon(1+A)$. Therefore,

$$\begin{aligned}\Delta v_{\theta_T}^{\bullet} &= \frac{1}{T^{\bullet}} \int_{t^{\bullet}}^{t^{\bullet}+T^{\bullet}} \left\{ \sum_{m=1}^{M} \frac{(-1)^{m+1}}{m} g\left(m, r^{\bullet}, \tau\right) \left(\varepsilon\left(m, r^{\bullet}, \tau\right) + f\left(m, \tau\right) \right) \sin\left(\varphi_m(\tau)\right) \right\} d\tau \\ &\approx \frac{1}{T^{\bullet}} \cdot g\left(r^{\bullet}, t^{\bullet}\right) \cdot \overline{\sin\left(\varphi_m(\tau)\right)} \cdot \overline{\sum_{m=1}^{M} \frac{(-1)^{m+1}}{m} \left(\varepsilon\left(m, r^{\bullet}, \tau\right) + f\left(m, \tau\right) \right)} \cdot T^{\bullet} \\ &\approx \frac{2}{\pi} \eta_{\varepsilon} \cdot (1 + A) g\left(r^{\bullet}, t^{\bullet}\right) \end{aligned} \tag{57}$$

Note that, in the above, the aggregate modal contribution of $g\left(m, r^{\bullet}, \tau\right)$ has been assumed, for the purposes of the estimating the mean flow characteristics, to be reasonably approximated by considering its non-modal form, $g\left(r^{\bullet}, \tau\right)$, Eq. 41.

$$\begin{aligned}\Delta v_{\theta_T}^{\bullet} &\approx \frac{2}{\pi} \eta_{\varepsilon} \cdot (1 + A) g\left(r^{\bullet}, t^{\bullet}\right) \\ &\approx \frac{2}{\pi} \eta_{\varepsilon} \cdot (1 + A) \frac{\eta \cdot \varsigma(A)}{r^{\bullet} v_{\theta}^{\bullet}} \\ &\approx \frac{2}{\pi} \eta \eta_{\varepsilon} \cdot (1 + A) \frac{\varsigma(A)}{r^{\bullet} \left(v_{\theta_L}^{\bullet} + \Delta v_{\theta_T}^{\bullet} \right)} \end{aligned} \tag{58}$$

The two constants/parameters η and η_{ε} could be subsumed into one parameter, but are kept distinct in the following analysis for the objective of preserving clarity with earlier analysis in the paper.

The result for the turbulent contribution to the mean tangential velocity profile (and the mean tangential vorticity) is an unexpected quadratic polynomial solution, thus suggesting that are two real possible solutions to the mean turbulent flow.

$$\Delta v_{\theta_T}^{\bullet} \approx \frac{1}{2} \left\{ \pm \sqrt{\left(\left(v_{\theta_L}^{\bullet} \right)^2 + \frac{8 \eta \eta_{\varepsilon}}{\pi} \cdot \frac{\varsigma(A)}{r^{\bullet}} (1 + A) \right)} - v_{\theta_L}^{\bullet} \right\} \tag{59}$$

The physically meaningful solution is

$$\Delta v_{\theta_T}^{\bullet} \approx \frac{1}{2} \left\{ \sqrt{\left(\left(v_{\theta_L}^{\bullet} \right)^2 + \frac{8 \eta \eta_{\varepsilon}}{\pi} \cdot \frac{\varsigma(A)}{r^{\bullet}} (1 + A) \right)} - v_{\theta_L}^{\bullet} \right\} \tag{60}$$

Not only does the introduction of the term $(1 + A)$, embodied in the definition of the $\varepsilon\left(m, r^{\bullet}, \tau\right)$ function, eliminate any form of singularity for $\Delta v_{\theta_T}^{\bullet}$ but it also insures that $\Delta v_{\theta_T}^{\bullet} \to 0$ as $r^{\bullet} \to 0$. Note that absolute- or RMS-value tangential turbulence parameter, η_{ε}, can be derived from empirical observations, if need be. The η_{ε} parameter is, in general, time-dependent. The following approximation can be used to estimate η_{ε}.

$$\eta_\varepsilon \propto \aleph \cdot \left(e^{-at^\bullet} - e^{-bt^\bullet} \right)$$
$$\downarrow \qquad (61a\text{-}b)$$
$$\eta_\varepsilon \approx \vartheta \cdot f\left(1, t^\bullet\right)$$

Where the exponential constants must satisfy the constraint $b > a$ and, further, a new constant/parameter, $\aleph$, has been introduced to help prescribe the anticipated "peak" tangential turbulence implicit in the mean flow profile. Alternatively, an approximate dependence between the parameter η_ε, the turbulence skew/offset constant ϑ, and the first (dominant) radial mode $f\left(1, t^\bullet\right)$ can be established. Finally, it is important to re-emphasize at this point that the turbulent contribution to the vortex mean flow also influences the turbulent fluctuation solutions via the A, B, and C parameters employed in the turbulent fluctuation governing equations, Eq. 15a-c. Thus the mean flow and the turbulent fluctuation solutions are based on coupled, and not independent, sets of equations. Therefore, the both sets of solutions need to be iterated upon together until satisfactory convergence is achieved.

Equations 60-61 provide an approximate analytic solution of the tangential velocity mean flow distribution. A direct numerical solution of Eq. 53 could also be performed so as to arrive at a nominally more accurate estimation of the profile. The same general type of mean-value approximations that were used to define the mean-flow expression for the tangential velocity distribution can also be employed to derive absolute expressions for the turbulence and Reynolds shear stress distributions. Note, also, a nuance is suggested in which for the definition/derivation of the Reynolds shear stresses it is assumed that each modal component of the two fluctuation velocities are multiplied together to yield a modal product before summation to yield an aggregate quantity. In this manner, it is insured that $\left|\overline{\hat{v}_r^\bullet \hat{v}_z^\bullet}\right| \neq \left|\overline{\hat{v}_r^\bullet}\right| \cdot \left|\overline{\hat{v}_z^\bullet}\right|$, etc., which is consistent with physical observations. The resulting expressions are

$$\left|\overline{\hat{v}_r^\bullet}\right| = \frac{1}{\pi^2}\left\{\sum_{m=1}^{M} \frac{(-1)^{m+1}}{m} g\left(m, r^\bullet, t^\bullet\right) \bar{f}\left(m, t^\bullet\right)\right\}$$

$$\left|\overline{\hat{v}_\theta^\bullet}\right| = \frac{1}{\pi^2}\left\{\sum_{m=1}^{M} \frac{(-1)^{m+1}}{m} g\left(m, r^\bullet, t^\bullet\right)\left[\varepsilon\left(m, r^\bullet, t^\bullet\right) + \bar{f}\left(m, t^\bullet\right)\right]\right\}$$

$$\left|\overline{\hat{v}_z^\bullet}\right| = \frac{1}{\pi^2}\left\{\sum_{m=1}^{M} \frac{(-1)^{m+1}}{m} h\left(m, r^\bullet, t^\bullet\right) \bar{f}\left(m, t^\bullet\right)\right\}$$

$$\left|\overline{\hat{v}_r^\bullet \hat{v}_z^\bullet}\right| = \frac{1}{\pi^4}\left\{\sum_{m=1}^{M} \frac{1}{m^2} g\left(m, r^\bullet, t^\bullet\right) h\left(m, r^\bullet, t^\bullet\right) \bar{f}\left(m, t^\bullet\right)^2\right\}$$

$$\left|\overline{\hat{v}_r^\bullet \hat{v}_\theta^\bullet}\right| = \frac{1}{\pi^4}\left\{\sum_{m=1}^{M} \frac{1}{m^2} g\left(m, r^\bullet, t^\bullet\right)^2 \bar{f}\left(m, t^\bullet\right)\left[\varepsilon\left(m, r^\bullet, t^\bullet\right) + \bar{f}\left(m, t^\bullet\right)\right]\right\}$$

$$\left|\overline{\hat{v}_z^\bullet \hat{v}_\theta^\bullet}\right| = \frac{1}{\pi^4}\left\{\sum_{m=1}^{M} \frac{1}{m^2} g\left(m, r^\bullet, t^\bullet\right) h\left(m, r^\bullet, t^\bullet\right) \bar{f}\left(m, t^\bullet\right)\left[\varepsilon\left(m, r^\bullet, t^\bullet\right) + \bar{f}\left(m, t^\bullet\right)\right]\right\}$$

$$TKE = \left(\left|\overline{\hat{v}_r^{\bullet}}\right|\right)^2 + \left(\left|\overline{\hat{v}_\theta^{\bullet}}\right|\right)^2 + \left(\left|\overline{\hat{v}_z^{\bullet}}\right|\right)^2$$

Where

$$\bar{f}\left(m,t^{\bullet}\right) \equiv \sum_{n=1}^{N} \alpha_{mn}\left(e^{-a_{mn}t^{\bullet}} - e^{-b_{mn}t^{\bullet}}\right)$$

(62a-h)

The mean flow and turbulent fluctuation solutions are not yet complete, though. The current formulation does not constrain the flow to having conserved or decreasing total kinetic/mechanical energy with time. In fact, the opposite is true; currently the analysis results in a large initial growth in total kinetic/mechanical energy for the vortex. This is, of course, not physically realizable. To address this problem it is necessary to introduce the concept of "accelerated aging" of the vortex when in a state of both transition and fully developed turbulent flow. This accelerated aging comes in the form of defining an "effective time" in the form of $t_{eff}^{\bullet} \approx \delta t^{\bullet}$ where δ is a constant such that $\delta \geq 1$. Note that this constant is analogous to the Squire constant, e.g. Ref. 20 and 23, though no assumptions as to eddy viscosity functionality need be made. Consequently, in comparing laminar and turbulent vortices, a laminar vortex flow characteristics would be evaluated at time $t^{\bullet}$ and a turbulent vortex would be evaluated at time $t_{eff}^{\bullet}$ for a physically realistic comparison to be made. There is no definitive approach that suggests itself so as to determine this vortex "aging" constant. Conservation of total kinetic energy, i.e. the total energy being constant, cannot be assumed because of viscous dissipation of such energy. It would seem, as a minimum, though, that an inequality relationship of the following form could be posited.

$$\int_0^{\infty} r^{\bullet}\left(v_{\theta_L}^{\bullet}\right)^2 dr^{\bullet}\Big|_{t^{\bullet}} \geq \int_0^{\infty} r^{\bullet}\left\{\left(v_{\theta_L}^{\bullet}\right)^2 + \overline{\left(\hat{v}_r^{\bullet}\right)^2} + \overline{\left(\hat{v}_\theta^{\bullet}\right)^2} + \overline{\left(\hat{v}_z^{\bullet}\right)^2}\right\} dr^{\bullet}\Big|_{t_{eff}^{\bullet}}$$

(63)

It is further conjectured that a specific limiting case of vortex kinetic energy "conservation" is of particular interest. This limiting case is as follows

$$\int_0^{\infty} r^{\bullet}\left(v_{\theta_L}^{\bullet}\right)^2 dr^{\bullet}\Big|_{t^{\bullet}} \approx \int_0^{\infty} r^{\bullet}\left(v_{\theta_L}^{\bullet} + 2\Delta v_{\theta_T}^{\bullet}\right)^2 dr^{\bullet}\Big|_{t_{eff}^{\bullet}}$$

(64)

Admittedly there is more artifice than rigor to the above relationship, but, as will be seen, the net result is an important insight into turbulent vortex evolution. What perhaps provides Eq. 64 its greatest utility, though, is that it makes the subsequent mathematical analysis very tractable. Making the appropriate substitutions, the following expression is yielded

$$\int_0^{\infty} r^{\bullet}\left(v_{\theta_L}^{\bullet}\right)^2 dr^{\bullet}\Big|_{t^{\bullet}} \approx \int_0^{\infty} r^{\bullet}\left\{\left(v_{\theta_L}^{\bullet}\right)^2 + \frac{8\eta\eta_{\varepsilon}}{\pi}\cdot\frac{\varsigma(A)}{r^{\bullet}}(1+A)\right\} dr^{\bullet}\Big|_{t_{eff}^{\bullet}}$$

(65)

The integration of the rightmost term can be approximated by means of the mean value theorem of calculus whereby the following holds: $\int_0^{\infty}(1+A)dr^{\bullet} \approx r^{\bullet}/2\Big|_0^{2r_c^{\bullet}\left(t_{eff}^{\bullet}\right)} = r_c^{\bullet}\left(t_{eff}^{\bullet}\right)$. Implicit in this resulting expression is that: (1) as $r^{\bullet} = 0$ then $A \to -1$, (2) as $r^{\bullet} \to r_c^{\bullet}\left(t_{eff}^{\bullet}\right)$ then $A \to -1/2$, (3) A is

approximately symmetrical about $r^\bullet = r_c^\bullet\left(t_{eff}^\bullet\right)$ and so integration can be bounded within an upper limit of $2r_c^\bullet\left(t_{eff}^\bullet\right)$, and (4) $\varsigma(A) \approx 1$ for the range $0 \le r^\bullet \le 2r_c^\bullet\left(t_{eff}^\bullet\right)$. Therefore, Eq. 65 becomes

$$\int_0^\infty r^\bullet\left(v_{\theta_L}^\bullet\right)^2 dr^\bullet\Big|_{t^\bullet} \approx \int_0^\infty r^\bullet\left(v_{\theta_L}^\bullet\right)^2 dr^\bullet\Big|_{t_{eff}^\bullet} + \frac{8\eta\eta_\varepsilon}{\pi} r_c^\bullet\left(t_{eff}^\bullet\right) \tag{66}$$

Next assume that the mean tangential velocity profile can be approximated by the Lamb-Oseen profile, i.e. $v_{\theta_L}^\bullet \approx \left(1/r^\bullet\right)\left(1-\exp\left(-\left(r^\bullet\right)^2/4t^\bullet\right)\right)$ for $t^\bullet >> 0$. Making this substitution yields the following

$$\int_0^\infty \frac{1}{r^\bullet}\left(1-\exp\left(-\left(r^\bullet\right)^2/4t^\bullet\right)\right)^2 dr^\bullet \approx \int_0^\infty \frac{1}{r^\bullet}\left\{\left(1-\exp\left(-\left(r^\bullet\right)^2/4t_{eff}^\bullet\right)\right)^2\right\} dr^\bullet + \frac{8\eta\eta_\varepsilon}{\pi} r_c^\bullet\left(t_{eff}^\bullet\right) \tag{67}$$

Equation 67 has solutions in terms of exponential integrals. Therefore, integrating and simplifying

$$\left\{\frac{1}{2}Ei\left(-\left(r^\bullet\right)^2/2t^\bullet\right) - Ei\left(-\left(r^\bullet\right)^2/4t^\bullet\right)\right\}\Big|_0^\infty \approx \left\{\frac{1}{2}Ei\left(-\left(r^\bullet\right)^2/2t_{eff}^\bullet\right) - Ei\left(-\left(r^\bullet\right)^2/4t_{eff}^\bullet\right)\right\}\Big|_0^\infty + \frac{8\eta\eta_\varepsilon}{\pi} r_c^\bullet\left(t_{eff}^\bullet\right) \tag{68}$$

Note that $Ei(-\infty) = 0$ and $Ei(0) = -\infty$, e.g. Ref. 27. This latter singularity of $Ei(x)$ has to be handled with caution. Or

$$Lim_{r^\bullet \to 0^-}\left\{\frac{1}{2}\left[Ei\left(-\left(r^\bullet\right)^2/2t_{eff}^\bullet\right) - Ei\left(-\left(r^\bullet\right)^2/2t^\bullet\right)\right] - \left[Ei\left(-\left(r^\bullet\right)^2/4t_{eff}^\bullet\right) - Ei\left(-\left(r^\bullet\right)^2/4t^\bullet\right)\right]\right\} \approx \frac{8\eta\eta_\varepsilon}{\pi} r_c^\bullet\left(t_{eff}^\bullet\right) \tag{69}$$

The limiting value of the left-hand-side of Eq. 69 as $r^\bullet \to 0^-$ needs to be determined. This can be established by noting that $Ei(x) = C + (1/2)\ln(-x) + \sum_{k=1}^\infty x^k/k\cdot k!$ for $x < 0$, where C is the Euler constant, e.g. Ref. 14. Further, note that $\sum_{k=1}^\infty x^k/k\cdot k! \to 0$ as $x \to 0$. Therefore, this implies that $Ei(x) \to C + (1/2)\ln(-x)$ as $x \to 0^-$. Making this substitution into Eq. 69 gives

$$\frac{1}{2}\ln\left(t^\bullet/t_{eff}^\bullet\right) - \ln\left(t^\bullet/t_{eff}^\bullet\right) = \ln\left(\sqrt{t_{eff}^\bullet/t^\bullet}\right) \approx \frac{8\eta\eta_\varepsilon}{\pi} r_c^\bullet\left(t_{eff}^\bullet\right) \tag{70}$$

Recasting the above equation yields the following quasi-linear relationship between $t_{eff}^\bullet$ and $t^\bullet$.

$$t_{eff}^\bullet \approx \exp\left(\frac{16\eta\eta_\varepsilon}{\pi} r_c^\bullet\left(t_{eff}^\bullet\right)\right)\cdot t^\bullet \tag{71}$$

Assume that the vortex core radius can be approximated by the relationship $r_c^{\bullet}\left(t_{eff}^{\bullet}\right) \approx \sqrt{1+4\alpha_L t_{eff}^{\bullet}}$, where $\alpha_L = 1.25643...$ is the Lamb constant, e.g. Ref. 23. Therefore, making this final substitution/approximation gives

$$t_{eff}^{\bullet} \approx \exp\left(\frac{16\eta\eta_\varepsilon}{\pi}\sqrt{1+4\alpha_L t_{eff}^{\bullet}}\right)\cdot t^{\bullet} \tag{72}$$

For small values of nondimensional time, the above relationship yields a Squire-like (Refs. 20 and 23) near-constant ratio of apparent to actual viscosity to account for turbulent flow effects on the time evolution of the turbulent mean flow characteristics of a line vortex, i.e., $t_{eff}^{\bullet} \to \delta t^{\bullet}$ for $t^{\bullet} \to 0$ where $\delta \approx \exp\left(16\eta\eta_\varepsilon/\pi\right)$. As time increases, though, significant nonlinear effects have to be accounted for in the evolution of the turbulent vortex. Further, it must be pointed out that even at small values of nondimensional time "δ" is not an actual constant, this is because the parameter η_ε has its own time dependence, Eq. 61. For example, when $t^{\bullet} = 0$, and the vortex is in its initial laminar flow state, then $\eta_\varepsilon = 0$ and, therefore, as required for fully laminar flow, $\delta = 1$, given the above derived Eq. 72.

This concludes the discussion in this paper of the turbulent flow contribution for a line vortex. The analysis to this point can only be considered phenomenological in nature. This both the consequence of the approximations employed in the analysis as well as, most importantly, the lack of a rigorous methodology defined so far as to definitively assigning values to the large set of coefficients and constants embodied in the analytical treatment. It is likely that a combination of invariant quantities, new conservation laws, and, inevitably, some amount of empiricism will be required to transform this phenomenological analysis to a truly predictive model. The analytical derivation of the laminar basic flow solution will next be summarized in Appendix B.

Appendix B – Summary of Laminar/Basic-Flow Solution

A laminar basic flow solution was derived in Ref. 4 that describes an initially Rankine-like vortex which evolves with time to a Lamb-Oseen profile. This solution was originally derived to study the vortex reconnection problem. However, it also defines an exact laminar solution for a columnar vortex with an initially uniform core axial vorticity distribution. This derivation will be summarized herein this appendix. Considering a point source formulation (in polar/cylindrical coordinates) of the problem, which is

$$\omega_z\Big|_{\substack{Finite\text{-}Core\\Filaments}} = \frac{1}{\pi r_{c0}^2}\int_0^{r_{c0}}\int_0^{2\pi}\left\{\int_s^{\infty}\omega_z\Big|_{Point\text{-}Source}dz_* + \int_{-\infty}^{-s}\omega_z\Big|_{Point\text{-}Source}dz_*\right\}d\theta_* dr_* \tag{73}$$

Where, from Ref. 9, the following holds

$$\omega_z\Big|_{Point\text{-}Source} = \frac{\gamma r_*}{8\sqrt{(\pi\nu t)^3}}e^{-\left\{\left(r^2+r_*^2-2rr_*\cos\theta_*\right)+\left(z-z_*\right)^2\right\}/4\nu t} \tag{74}$$

A line source expression can be defined as such

$$\omega_z\big|_{Line\text{-}Source} = \int_{s}^{\infty} \omega_z\big|_{Point\text{-}Source}\, dz_* + \int_{-\infty}^{-s} \omega_z\big|_{Point\text{-}Source}\, dz_*$$
$$= \frac{\gamma r_*}{8\pi\nu t}\left\{erfc\left(\frac{s-z}{\sqrt{4\nu t}}\right) + erfc\left(\frac{s+z}{\sqrt{4\nu t}}\right)\right\} e^{-\left(r^2+r_*^2-2rr_*\cos\theta_*\right)/4\nu t} \tag{75}$$

Substituting this line source expression, Eq. 75, into Eq. 73 gives

$$\omega_z = \frac{\gamma}{8\left(\pi r_{c0}\right)^2\nu t}\left\{erfc\left(\frac{s-z}{\sqrt{4\nu t}}\right) + erfc\left(\frac{s+z}{\sqrt{4\nu t}}\right)\right\} \int_0^{r_{c0}} \int_0^{2\pi} r_* e^{-\left(r^2+r_*^2-2rr_*\cos\theta_*\right)/4\nu t}\, d\theta_* dr_* \tag{76}$$

Also, from Ref. 9, the integration with respect to θ_* follows

$$\omega_z = \frac{\gamma}{4\pi r_{c0}^2\nu t}\left\{erfc\left(\frac{s-z}{\sqrt{4\nu t}}\right) + erfc\left(\frac{s+z}{\sqrt{4\nu t}}\right)\right\} \int_0^{r_{c0}} I_0\left(\frac{rr_*}{2\nu t}\right) \cdot r_* e^{-\left(r^2+r_*^2\right)/4\nu t} dr_* \tag{77}$$

Not unexpectedly, because of the problem being cast in polar/cylindrical coordinates, a modified Bessel function of the first kind of zero[th] order, $I_0(x)$, manifests itself in the above expression. The final form of axial vorticity solution will be expressed in terms of a series expansion of elemental functions. Noting from Ref. 9, for example, the following series definition of the modified Bessel function

$$I_v(z) = \sum_{r=0}^{\infty} \frac{(z/2)^{v+2r}}{r!\,\Gamma(v+r+1)} \qquad \text{Or} \qquad I_0(z) = \sum_{r=0}^{\infty} \frac{(z/2)^{2r}}{r!\,\Gamma(r+1)} \tag{78a-b}$$

Substituting the above modified Bessel series expression into Eq. 77

$$\omega_z = \frac{\gamma}{4\pi r_{c0}^2\nu t} e^{-r^2/4\nu t}\left\{erfc\left(\frac{s-z}{\sqrt{4\nu t}}\right) + erfc\left(\frac{s+z}{\sqrt{4\nu t}}\right)\right\} \int_0^{r_{c0}} e^{-r_*^2/4\nu t} \cdot \sum_{n=0}^{\infty} \frac{\left(r/4\nu t\right)^{2n} r_*^{2n+1}}{n!\,\Gamma(n+1)} dr_* \tag{79}$$

Noting the following integral formula from Ref. 13

$$\int x^{2m+1} e^{-a^2x^2} dx = -\frac{x^{2m} e^{-a^2x^2}}{2a^2} \cdot \sum_{k=0}^{m} \frac{m!}{(m-k)!\,(ax)^{2k}} \tag{80}$$

Then the following holds

$$\omega_z = \frac{-\gamma}{4\pi r_{c0}^2\nu t} e^{-r^2/4\nu t}\left\{erfc\left(\frac{s-z}{\sqrt{4\nu t}}\right) + erfc\left(\frac{s+z}{\sqrt{4\nu t}}\right)\right\}$$
$$\cdot \left\{\sum_{n=0}^{\infty} \frac{r^{2n} r_*^{2n} e^{-r_*^2/4\nu t}}{2\Gamma(n+1)\left(4\nu t\right)^{2n-1}} \cdot \sum_{k=0}^{n} \frac{\left(2\sqrt{\nu t}/r_*\right)^{2k}}{(n-k)!}\right\}\Bigg|_0^{r_{c0}} \tag{81}$$

Or, defining the new function $E_0(a,r,t)$ and applying the integration limits yields

$$\omega_z = \frac{-\gamma}{4\pi r_{c0}^2 \nu t} e^{-r^2/4\nu t} \left\{ erfc\left(\frac{s-z}{\sqrt{4\nu t}}\right) + erfc\left(\frac{s+z}{\sqrt{4\nu t}}\right) \right\} \left\{ E_0(r_{c0},r,t) - E_0\left(0^+,r,t\right) \right\}$$

Where

$$E_0(a,r,t) = \sum_{n=0}^{\infty} \frac{r^{2n} a^{2n} e^{-a^2/4\nu t}}{2\Gamma(n+1)(4\nu t)^{2n-1}} \cdot \sum_{k=0}^{n} \frac{\left(2\sqrt{\nu t}/a\right)^{2k}}{(n-k)!}$$

(82a-b)

The derived solution provides accurate estimates of finite-core vortex filament vorticity for the assumed vortex core structure with uniform vorticity at $t = 0$.

Proceeding next with the tangential velocity expression derivation, the tangential velocity is given by the following general equation

$$v_\theta \approx \left\{ \int Q(r) e^{\int P(r)dr} dr + C \right\} e^{-\int P(r)dr}$$

Where, in this particular case,

$$P(r) = 1/r$$

$$Q(r) = \frac{-\gamma}{4\pi r_{c0}^2 \nu t} e^{-r^2/4\nu t} \left\{ erfc\left(\frac{s-z}{\sqrt{4\nu t}}\right) + erfc\left(\frac{s+z}{\sqrt{4\nu t}}\right) \right\} \left\{ E_0(r_{c0},r,t) - E_0\left(0^+,r,t\right) \right\}$$

(83a-b)

The following holds

$$v_\theta = \frac{1}{r}\left(C + \int rQ(r)dr \right)$$

Which gives

$$v_\theta = \frac{1}{r} \left\{ C - \frac{\gamma}{4\pi r_{c0}^2 \nu t} \left(E_1(r_{c0},r,t) - E_1\left(0^+,r,t\right) \right) \left\{ erfc\left(\frac{s-z}{\sqrt{4\nu t}}\right) + erfc\left(\frac{s+z}{\sqrt{4\nu t}}\right) \right\} \right\}$$

(84a-b)

Where

$$E_1(a,b,t) \equiv \int_0^r \left\{ \sum_{n=0}^{\infty} r^{2n+1} e^{-r^2/4\nu t} \cdot \frac{a^{2n} e^{-a^2/4\nu t}}{2\Gamma(n+1)(4\nu t)^{2n-1}} \cdot \sum_{k=0}^{n} \frac{\left(2\sqrt{\nu t}/a\right)^{2k}}{(n-k)!} \right\} dr$$

(85)

Or, performing the required integration yields

$$E_1(a,b,t) \equiv \left\{ \sum_{n=0}^{\infty} \left(E_{10}(n,b,t) - E_{10}\left(n,0^+,t\right) \right) \cdot \frac{a^{2n} e^{-a^2/4\nu t}}{2\Gamma(n+1)(4\nu t)^{2n-1}} \cdot \sum_{k=0}^{n} \frac{\left(2\sqrt{\nu t}/a\right)^{2k}}{(n-k)!} \right\}$$

Which, given the Eq. 80 integral formula, yields

$$E_{10}(n,c,t) = -2\nu t \cdot c^{2n} e^{-c^2/4\nu t} \cdot \sum_{j=0}^{n} \frac{n!}{(n-j)!} \left(\frac{2\sqrt{\nu t}}{c} \right)^{2j}$$

(86a-b)

Now noting that the integration constant, C, is derived by the boundary constraint that $v_\theta = 0$ at $r = 0$, therefore, the tangential velocity expression is given by

$$v_\theta = \frac{\gamma}{4\pi r_{c0}^2 \nu t r} \left\{ \left(E_1(r_{c0},0,t) - E_1\left(0^+,0,t\right) \right) - \left(E_1(r_{c0},r,t) - E_1\left(0^+,r,t\right) \right) \right\} \cdot \left\{ erfc\left(\frac{s-z}{\sqrt{4\nu t}} \right) + erfc\left(\frac{s+z}{\sqrt{4\nu t}} \right) \right\}$$

(87)

Equations 82 and 87, the axial vorticity and the tangential velocity expressions, also provide an alternate model for an unsteady monopolar/columnar finite-core vortex filament. The above partial finite-core vortex filament reconnection analytical work leads to expressions (for the case where $s = 0$) that define a laminar, unsteady, two-dimensional finite-core vortex model that has an initially uniform axial vorticity in the vortex core. The axial vorticity and tangential velocity distributions for this vortex model are given by the expressions noted below and follow simply from the work presented earlier:

$$\omega_z = \frac{-\gamma}{2\pi r_{c0}^2 \nu t} e^{-r^2/4\nu t} \left\{ E_0(r_{c0},r,t) - E_0\left(0^+,r,t\right) \right\}$$

And

$$v_\theta = \frac{\gamma}{2\pi r_{c0}^2 \nu t r} \left\{ \left(E_1(r_{c0},0,t) - E_1\left(0^+,0,t\right) \right) - \left(E_1(r_{c0},r,t) - E_1\left(0^+,r,t\right) \right) \right\}$$

(88a-b)

Note that, of course, $v_z = v_r = 0$ for this vortex model. In this model the vortex tangential velocity distribution transitions from a Rankine-like profile to a Lamb-Oseen-like profile as time progresses. Because of numerical stability issues at very small values of time, $t \to 0$, the alternate asymptotic expressions should be used for $t = 0$.

$$\omega_z = \frac{\gamma}{\pi r_{c0}^2} u\left(1 - \frac{r}{r_{c0}} \right)$$

$$v_\theta = \frac{\gamma}{2\pi r_{c0}} \left\{ \frac{r}{r_{c0}} u\left(1 - \frac{r}{r_{c0}} \right) + \frac{r_{c0}}{r} \left\{ 1 - u\left(1 - \frac{r}{r_{c0}} \right) \right\} \right\}$$

(89a-b)

The Aboelkassem model (Ref. 8) and the above uniform finite-core laminar vortex model all transition from a Rankine-like initial tangential velocity profile to a Lamb-Oseen profile over time. They are two mathematically distinct but essentially functionally equivalent solutions.

Appendix C – Assessment of the Approximation Implicit in the Analysis and Derivation of an Equation Critical to Defining the Axial Turbulent Fluctuation

The semi-arbitrary functional relationship, Eq. 37b, for the $h\left(r^\bullet, t^\bullet\right)$ needs to be augmented with a more precise means of derivation, this will be accomplished by considering the vorticity component definitions

directly. In addition, the level of approximation in the turbulent fluctuation vorticity estimates for $\hat{v}_r^{\bullet}$, $\hat{v}_\theta^{\bullet}$ and $\hat{v}_z^{\bullet}$ will be qualitatively assessed by making the appropriate substitutions into these vorticity/velocity relationships. In the analysis shown below it is first assumed that the implied functional relationships in these vorticity definitions are equally applicable to turbulent vorticity fluctuations. Then the appropriate substitutions from previous work were made with respect to the derived intermediate forms of the turbulent fluctuation solutions. Then the higher-mode continuity constraints are applied such that $\sum_{m=1}^{\infty^-} a \cdot mf_m\left(t^{\bullet}\right) \to 0$. Therefore, the following must hold true

$$
\begin{gathered}
\omega_r = \frac{1}{r}\frac{\partial v_z}{\partial \theta} - \frac{\partial v_\theta}{\partial z} \\
\downarrow \\
\hat{\omega}_r^{\bullet} = \frac{1}{r^{\bullet}}\frac{\partial \hat{v}_z^{\bullet}}{\partial \theta} - \frac{\partial \hat{v}_\theta^{\bullet}}{\partial z^{\bullet}} \\
\downarrow \\
-\frac{\hat{v}_r^{\bullet}}{\ell^{\bullet}} \approx -\frac{1}{\ell^{\bullet}}\left\{\sum_{m=1}^{M}\chi(m)g\left(m,r^{\bullet},t^{\bullet}\right)f\left(m,t^{\bullet}\right)\sin\left(m\left(\theta - z^{\bullet}/A\right)+\varphi_m\left(t^{\bullet}\right)\right)\right\} \\
\approx \frac{1}{r^{\bullet}}\frac{\partial}{\partial\theta}\left\{\sum_{m=1}^{M}\chi(m)\left(h\left(r^{\bullet},t^{\bullet}\right)-g\left(m,r^{\bullet},t^{\bullet}\right)C\theta\right)f\left(m,t^{\bullet}\right)\sin\left(m\left(\theta - z^{\bullet}/A\right)+\varphi_m\left(t^{\bullet}\right)\right)\right\} \\
-\frac{\partial}{\partial z^{\bullet}}\left\{\sum_{m=1}^{M}\chi(m)g\left(m,r^{\bullet},t^{\bullet}\right)\left(\varepsilon\left(m,r^{\bullet},t^{\bullet}\right)+f\left(m,t^{\bullet}\right)(1-B\theta)\right)\sin\left(m\left(\theta - z^{\bullet}/A\right)+\varphi_m\left(t^{\bullet}\right)\right)\right\} \\
\downarrow \\
\sum_{m=1}^{M}\chi(m)g\left(m,r^{\bullet},t^{\bullet}\right)f\left(m,t^{\bullet}\right)\sin\left(m\left(\theta - z^{\bullet}/A\right)+\varphi_m\left(t^{\bullet}\right)\right) \approx \\
-\frac{C}{r^{\bullet}}\left\{\sum_{m=1}^{M}\chi(m)g\left(m,r^{\bullet},t^{\bullet}\right)f\left(m,t^{\bullet}\right)\sin\left(m\left(\theta - z^{\bullet}/A\right)+\varphi_m\left(t^{\bullet}\right)\right)\right\} \\
+\frac{1}{r^{\bullet}}\left\{\sum_{m=1}^{M}m\cdot\chi(m)\left(h\left(r^{\bullet},t^{\bullet}\right)-g\left(m,r^{\bullet},t^{\bullet}\right)C\theta\right)f\left(m,t^{\bullet}\right)\cos\left(m\left(\theta - z^{\bullet}/A\right)+\varphi_m\left(t^{\bullet}\right)\right)\right\} \\
+\frac{1}{A}\left\{\sum_{m=1}^{M}m\cdot\chi(m)g\left(m,r^{\bullet},t^{\bullet}\right)\left(\varepsilon\left(m,r^{\bullet},t^{\bullet}\right)+f\left(m,t^{\bullet}\right)(1-B\theta)\right)\cos\left(m\left(\theta - z^{\bullet}/A\right)+\varphi_m\left(t^{\bullet}\right)\right)\right\} \\
\downarrow \\
C \approx -r^{\bullet}
\end{gathered}
\tag{90}
$$

The above equation can only be exactly satisfied by a specific constraint – and/or test of approximation – on the mean flow parameter C. This constraint cannot be universally satisfied, and, so, the above result suggests that one of the fundamental approximations used to derive the turbulent fluctuation governing equations, that of $\hat{v}_r \approx -\ell\hat{\omega}_r$ is fairly accurate in the inner-core of the vortex, i.e. $r < r_c(t)$, but is less valid for the outer-core of the vortex, as has been confirmed numerically. Fortunately, the inner-core is where the bulk of the vortex turbulence is located.

$$\hat{\omega}_\theta^\bullet = \frac{\partial \hat{v}_r^\bullet}{\partial z^\bullet} - \frac{\partial \hat{v}_z^\bullet}{\partial r^\bullet}$$

$$\downarrow$$

$$-\frac{\hat{v}_\theta^\bullet}{\ell^\bullet} \approx -\frac{1}{\ell^\bullet}\left\{\sum_{m=1}^{M}\chi(m)g\left(m,r^\bullet,t^\bullet\right)\left(\varepsilon\left(m,r^\bullet,t^\bullet\right)+f\left(m,t^\bullet\right)(1-B\theta)\right)\sin\left(m\left(\theta-z^\bullet/A\right)+\varphi_m\left(t^\bullet\right)\right)\right\}$$

$$\approx \frac{\partial}{\partial z^\bullet}\left\{\sum_{m=1}^{M}\chi(m)g\left(m,r^\bullet,t^\bullet\right)f\left(m,t^\bullet\right)\sin\left(m\left(\theta-z^\bullet/A\right)+\varphi_m\left(t^\bullet\right)\right)\right\}$$

$$-\frac{\partial}{\partial r^\bullet}\left\{\sum_{m=1}^{M}\chi(m)\left(h\left(r^\bullet,t^\bullet\right)-g\left(m,r^\bullet,t^\bullet\right)C\theta\right)f\left(m,t^\bullet\right)\sin\left(m\left(\theta-z^\bullet/A\right)+\varphi_m\left(t^\bullet\right)\right)\right\}$$

$$\downarrow$$

$$\sum_{m=1}^{M}\chi(m)g\left(m,r^\bullet,t^\bullet\right)\left(\varepsilon\left(m,r^\bullet,t^\bullet\right)+f\left(m,t^\bullet\right)(1-B\theta)\right)\sin\left(m\left(\theta-z^\bullet/A\right)+\varphi_m\left(t^\bullet\right)\right)\approx$$

$$-\frac{1}{A}\left\{\sum_{m=1}^{M}m\cdot\chi(m)g\left(m,r^\bullet,t^\bullet\right)f\left(m,t^\bullet\right)\cos\left(m\left(\theta-z^\bullet/A\right)+\varphi_m\left(t^\bullet\right)\right)\right\}$$

$$-\left\{\sum_{m=1}^{M}\chi(m)\left(\frac{\partial h}{\partial r^\bullet}-\left(\frac{\partial g}{\partial r^\bullet}C+g\frac{\partial C}{\partial r^\bullet}\right)\theta\right)f\left(m,t^\bullet\right)\sin\left(m\left(\theta-z^\bullet/A\right)+\varphi_m\left(t^\bullet\right)\right)\right\}$$

$$\downarrow$$

$$\begin{cases}(I) & C\dfrac{\partial}{\partial r^\bullet}g\left(m,r^\bullet,t^\bullet\right)+\left(\dfrac{\partial C}{\partial r^\bullet}+B\right)g\left(m,r^\bullet,t^\bullet\right)\approx 0\\[2ex] (II) & \dfrac{\partial}{\partial r^\bullet}h\left(r^\bullet,t^\bullet\right)+\left(1+\varepsilon\left(m,r^\bullet,t^\bullet\right)\Big/f\left(m,t^\bullet\right)\right)g\left(m,r^\bullet,t^\bullet\right)=0\\ & \rightarrow \dfrac{\partial}{\partial r^\bullet}h\left(m,r^\bullet,t^\bullet\right)+\left\{1+d_m\cdot(1+A)\right\}g\left(m,r^\bullet,t^\bullet\right)\approx 0\end{cases} \tag{91}$$

The analysis of the above vorticity relationship yields two results. The first result (*I*) can be used as an assessment of the level of approximation of assumed fundamental relationship $\hat{v}_\theta \approx -\ell\hat{\omega}_\theta$. The resultant constraint $C\left(\partial g/\partial r^\bullet\right)+\left(\partial C/\partial r^\bullet+B\right)g\approx 0$ is arrived by collecting the terms multiplied by θ. This resultant constraint is equivalent to the alternate constraint $g\propto -\exp\left(-\int(B/C)dr\right)\Big/C$. Both these versions of constraint cannot be universally satisfied, thereby confirming that $\hat{v}_\theta \approx -\ell\hat{\omega}_\theta$ is indeed only an approximation. This approximation is again valid primarily in the inner-core of the turbulent vortex, as has been confirmed numerically, wherein most of the vortex turbulence resides. In this regards the approximation $\hat{v}_\theta \approx -\ell\hat{\omega}_\theta$ continues to be deemed acceptable, as does the overall turbulent flow analysis. The second result (*II*) from the above analysis is the sought after more precise relationship defining $h\left(r^\bullet,t^\bullet\right)$. Note that a modal dependence is intrinsic to this function, i.e. $h\left(r^\bullet,t^\bullet\right)\rightarrow h\left(m,r^\bullet,t^\bullet\right)$. Further, the ratio of the functions $\varepsilon\left(m,r^\bullet,t^\bullet\right)$ and $f\left(m,t^\bullet\right)$ have been approximated by means of the introduction of the modal constants d_m as well as retention of the prescribed $(1+A)$ term for $\varepsilon\left(m,r^\bullet,t^\bullet\right)$.

$$\hat{\omega}_z^{\bullet} = \frac{\partial \hat{v}_\theta^{\bullet}}{\partial r^{\bullet}} + \frac{\hat{v}_\theta^{\bullet}}{r^{\bullet}} - \frac{1}{r^{\bullet}}\frac{\partial \hat{v}_r^{\bullet}}{\partial \theta}$$

$$\downarrow$$

$$-\frac{\hat{v}_z^{\bullet}}{\ell^{\bullet}} \approx -\frac{1}{\ell^{\bullet}}\left\{\sum_{m=1}^{M}\chi(m)\left(h\left(r^{\bullet},t^{\bullet}\right)-g\left(m,r^{\bullet},t^{\bullet}\right)C\theta\right)f\left(m,t^{\bullet}\right)\sin\left(m\left(\theta-z^{\bullet}/A\right)+\varphi_m\left(t^{\bullet}\right)\right)\right\}$$

$$\approx \frac{\partial}{\partial r^{\bullet}}\left\{\sum_{m=1}^{M}\chi(m)g\left(m,r^{\bullet},t^{\bullet}\right)\left(\varepsilon\left(m,r^{\bullet},t^{\bullet}\right)+f\left(m,t^{\bullet}\right)(1-B\theta)\right)\sin\left(m\left(\theta-z^{\bullet}/A\right)+\varphi_m\left(t^{\bullet}\right)\right)\right\}$$

$$+\frac{1}{r^{\bullet}}\left\{\sum_{m=1}^{M}\chi(m)g\left(m,r^{\bullet},t^{\bullet}\right)\left(\varepsilon\left(m,r^{\bullet},t^{\bullet}\right)+f\left(m,t^{\bullet}\right)(1-B\theta)\right)\sin\left(m\left(\theta-z^{\bullet}/A\right)+\varphi_m\left(t^{\bullet}\right)\right)\right\}$$

$$-\frac{1}{r^{\bullet}}\frac{\partial}{\partial\theta}\left\{\sum_{m=1}^{M}\chi(m)g\left(m,r^{\bullet},t^{\bullet}\right)f\left(m,t^{\bullet}\right)\sin\left(m\left(\theta-z^{\bullet}/A\right)+\varphi_m\left(t^{\bullet}\right)\right)\right\}$$

$$\downarrow$$

$$\sum_{m=1}^{M}\chi(m)\left(h\left(r^{\bullet},t^{\bullet}\right)-g\left(m,r^{\bullet},t^{\bullet}\right)C\theta\right)f\left(m,t^{\bullet}\right)\sin\left(m\left(\theta-z^{\bullet}/A\right)+\varphi_m\left(t^{\bullet}\right)\right)\approx$$

$$\sum_{m=1}^{M}\chi(m)\frac{\partial g}{\partial r^{\bullet}}\cdot\left(\varepsilon\left(m,r^{\bullet},t^{\bullet}\right)+f\left(m,t^{\bullet}\right)(1-B\theta)\right)\sin\left(m\left(\theta-z^{\bullet}/A\right)+\varphi_m\left(t^{\bullet}\right)\right)$$

$$+\sum_{m=1}^{M}\chi(m)g\left(m,r^{\bullet},t^{\bullet}\right)\left(\frac{\partial\varepsilon}{\partial r^{\bullet}}-f\left(m,t^{\bullet}\right)\frac{\partial B}{\partial r^{\bullet}}\theta\right)\sin\left(m\left(\theta-z^{\bullet}/A\right)+\varphi_m\left(t^{\bullet}\right)\right)$$

$$+\frac{1}{r^{\bullet}}\left\{\sum_{m=1}^{M}\chi(m)g\left(m,r^{\bullet},t^{\bullet}\right)\left(\varepsilon\left(m,r^{\bullet},t^{\bullet}\right)+f\left(m,t^{\bullet}\right)(1-B\theta)\right)\sin\left(m\left(\theta-z^{\bullet}/A\right)+\varphi_m\left(t^{\bullet}\right)\right)\right\}$$

$$-\frac{1}{r^{\bullet}}\left\{\sum_{m=1}^{M}m\cdot\chi(m)g\left(m,r^{\bullet},t^{\bullet}\right)f\left(m,t^{\bullet}\right)\cos\left(m\left(\theta-z^{\bullet}/A\right)+\varphi_m\left(t^{\bullet}\right)\right)\right\}$$

$$\downarrow$$

$$\begin{cases}(I) & \left(\dfrac{\partial g}{\partial r^{\bullet}}+\dfrac{g}{r^{\bullet}}\right)(1+\varepsilon/f)+g\dfrac{\partial\varepsilon}{\partial r^{\bullet}}-h=0 \\ & \qquad\qquad \rightarrow\left(\dfrac{\partial g}{\partial r^{\bullet}}+\dfrac{g}{r^{\bullet}}\right)(1+d_m)+g\dfrac{\partial\varepsilon}{\partial r^{\bullet}}-h\approx 0 \\ (II) & B\dfrac{\partial g}{\partial r^{\bullet}}+\left(\dfrac{\partial B}{\partial r^{\bullet}}+\dfrac{B}{r^{\bullet}}-C-\dfrac{\partial\varepsilon}{\partial r^{\bullet}}\right)g=0\end{cases}$$

(92a-c)

Collecting terms with and without θ as a multiplier yields two new constraints and/or tests for approximation. For brevity the following abbreviated nomenclature is used in defining the constraints: $\varepsilon \equiv \varepsilon\left(m,r^{\bullet},t^{\bullet}\right)$, $f \equiv f\left(m,t^{\bullet}\right)$, etc. These constraints, like the others before them, cannot be universally satisfied, and, so, the above results suggest that all of the fundamental approximations used to derive the turbulent fluctuation governing equations, including the last one $\hat{v}_z \approx -\ell\hat{\omega}_z$ are fairly accurate in the inner-core of the vortex, i.e. $r < r_c(t)$, but is less valid for the outer-core of the vortex. This result, like the others, has been confirmed numerically.